Large eddy simulation with modeled wall-stress: recent progress and future directions

Johan LARSSON*, Soshi KAWAI**, Julien BODART*** and Ivan BERMEJO-MORENO†
* Department of Mechanical Engineering, University of Maryland
College Park, MD, 20742, USA
E-mail: jola@umd.edu
** Department of Aerospace Engineering, Tohoku University
Sendai, Miyagi, 980-8579, Japan
E-mail: kawai@cfd.mech.tohoku.ac.jp
*** DAEP, ISAE-Supaero, Université de Toulouse
10 Avenue Edouard Belin, 31400 Toulouse, France
E-mail: julien.bodart@isae-supaero.fr
† Department of Aerospace and Mechanical Engineering, University of Southern California
Los Angeles, CA, 90089, USA
E-mail: bermejom@usc.edu

Received 30 July 2015

Abstract
The paper provides a brief introduction to the near-wall problem of LES and how it can be solved through modeling of the near-wall turbulence. The distinctions and key differences between different approaches are emphasized, both in terms of fidelity (LES, wall-modeled LES, and DES) and in terms of different wall-modeled LES approaches (hybrid LES/RANS and wall-stress-models). The focus is on approaches that model the wall-stress directly, i.e., methods for which the LES equations are formally solved all the way down to the wall. Progress over the last decade is reviewed, and the most important and promising directions for future research are discussed.

Key words : Large eddy simulation, Wall-bounded flows, Wall-model

1. Introduction

The large eddy simulation (LES) technique has now essentially displaced the Reynolds-averaged Navier Stokes (RANS) approach in the world of academic turbulence research. In practical engineering settings, however, the LES technique has made at most minor and partial inroads, being used in corporate research centers but rarely in the actual engineering design process. This situation is, in large part, due to the excessive computational cost of handling turbulent boundary layers. While boundary layers will always induce a significant computational cost regardless of how they are modeled (due to them being thin relative to other dimensions), the issue becomes acute at high Reynolds numbers.

There have been many different proposed solutions to this "near-wall problem of LES" over the last 50 years. A multitude of approaches have been suggested, using different arguments and with different objectives. They all aim to do the same thing: to model the turbulence in the inner part of the boundary layer, thus removing the need to resolve any turbulent eddies there. The methods differ in their treatment of the outer part of the boundary layer, specifically whether this is modeled (as it is in the original version of detached eddy simulation conceived by Spalart *et al.*, 1997, referred to in this paper as DES97) or resolved. The focus of this paper is on the latter category, i.e., methods that resolve the energetic motions in the outer boundary layer but treat them in a modeled, approximate fashion in the inner boundary layer. In this paper, we refer to such methods as "wall-modeled LES" or "WMLES". As will be described in section 2.3, we then divide wall-modeled LES into two sub-categories: (I) hybrid LES/RANS, and (II) wall-stress-modeled LES. The first era of wall-modeling, from the first paper by Deardorff (1970) to the end of the 1990s, focused almost exclusively

on wall-stress-modeling, the main exception being the brilliant paper by Schumann (1975) which contained the seeds of hybrid LES/RANS as well. Baggett (1998) and others started investigating the feasibility of the hybrid LES/RANS technique in the mid-to-late 1990s, which spurred a rapid growth in interest and proposed modeling combinations under this umbrella.

The state of the wall-modeling field up to the early-to-mid 2000s was reviewed quite comprehensively by Piomelli & Balaras (2002), Sagaut (2006), and Piomelli (2008). In addition, the state of DES (from DES97 and later modifications) was reviewed recently by Spalart (2009). The present paper builds on these prior reviews. We start by giving an overview and introduction to wall-modeled LES methods (both hybrid LES/RANS and wall-stress-models) in section 2. We then narrow our scope to focus exclusively on wall-stress-models in section 3, specifically on some important and interesting developments during the last decade.

2. Overview of wall-modeled LES (WMLES)

A turbulent boundary layer is truly a multi-scale phenomenon, and therein lies the (near-wall) problem. The turbulence kinetic energy is carried by eddies of different characteristic sizes in layers near and far from the wall, a fact which was nicely visualized by Jimenez (2012).

The wall-modeled LES philosophy is to respect this multi-scale nature of the boundary layer, by directly resolving the energetic eddies in the outer layer (where they are large) but instead to model all the energetic eddies in the inner layer (where they are small). Thus the entire inner-layer dynamics (streaks, quasi-streamwise vortices, peak production and dissipation, etc) are removed from the dynamical system and represented by a single value of the wall shear stress τ_w. This is a rather drastic truncation of the wall-turbulence dynamical system – as it has to be in order to drastically reduce the computational cost. Given the removal of the peak production region in the inner layer, one may wonder where the resolved outer-layer turbulence in wall-modeled LES comes from? The answer is simply that it is produced (and later dissipated) in the outer layer, exactly as it should be in high-Re wall-turbulence, where the Reynolds stresses have been found to be predominantly produced at the same wall distance as they are later dissipated (Hoyas & Jimenez, 2008).

2.1. Estimated grid requirements

It is very instructive to estimate the number of grid points required for LES of a canonical "unit" of a turbulent boundary layer: a cube of size δ^3 where δ is the local boundary layer thickness. This follows the classic works of Chapman (1979) and Spalart *et al.* (1997), but uses the updated skin-friction correlations of Choi & Moin (2012). The boundary layer has a friction Reynolds number $Re_\tau = \delta/l_v$, where the viscous length scale is $l_v = \nu/u_\tau$, ν is the kinematic viscosity, and $u_\tau = \sqrt{\tau_w/\rho}$ is the friction velocity defined from the wall stress τ_w and the density ρ.

In keeping with the multi-scale nature of a turbulent boundary layer, we estimate the grid requirements separately in the different layers. In the viscous layer (say $y^+ = y/l_v \lesssim 50$), a reasonable (but not excessively fine) LES grid would have $(\Delta x^+, \Delta z^+) \approx (40, 20)$ and a wall-normal grid-spacing varying approximately linearly from $\Delta y_w^+ \approx 1$ to $\Delta y^+ \approx 5$. In the outer layer (say $y/\delta \gtrsim 0.2$), a similarly reasonable grid would have $(\Delta x/\delta, \Delta z/\delta) \approx (0.08, 0.05)$ and $\Delta y/\delta$ varying linearly from 0.02 at $y/\delta = 0.2$ to 0.05 at the edge of the boundary layer (i.e., at $y = \delta$). At sufficiently high Reynolds numbers, an overlap layer (the "log-layer") develops between the viscous and outer layers; we take the grid-spacings to vary linearly in the log-layer in all three directions. The estimated number of grid points for LES in each layer is shown in Fig. 1(a).

The cost of the outer layer is independent of Re_τ, whereas both the viscous and logarithmic layers have costs that scale as $O(Re_\tau^2)$. This cost-scaling is the "near-wall problem of LES": it implies that the vast majority of computational resources will be spent on the viscous and logarithmic layers (i.e., the inner layer) at high Reynolds numbers. It also implies that LES is almost as costly as DNS for boundary layer flows.

A subtle point is that it is not just the viscous layer that causes this cost-scaling, but also the overlap (log-) layer; in fact, the latter was singled out in Fig. 1(a) specifically to make this point. The implication is that one must model both the viscous layer *and* most of the log-layer in order to break the Re-scaling of the computational cost. In practical terms, this means that the modeling interface *must* be defined in terms of outer units, i.e., as a fraction of δ.

To estimate the cost of wall-modeled LES (WMLES), we note that the outer layer must be resolved exactly as in standard LES. The question of the required resolution in the inner layer is quite straightforward for hybrid LES/RANS methods (no limit on wall-parallel Δx and Δz; resolve wall-normal Δy just like in RANS), but is deeper and more important than it appears at first sight for wall-stress-modeled LES. For these approaches, the inner layer is modeled, yet the LES is formally defined all the way to the wall, and therefore one has a doubly defined solution in the inner layer. The wall-

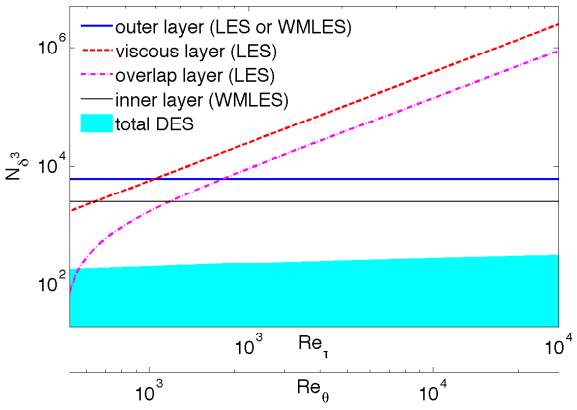

(a) Grid points in each separate layer: outer ($y/\delta \gtrsim 0.2$), viscous ($y^+ \lesssim 50$), overlap ($50 \lesssim y^+ \lesssim 0.2\delta^+$). Note that the viscous and overlap layers together form the inner layer.

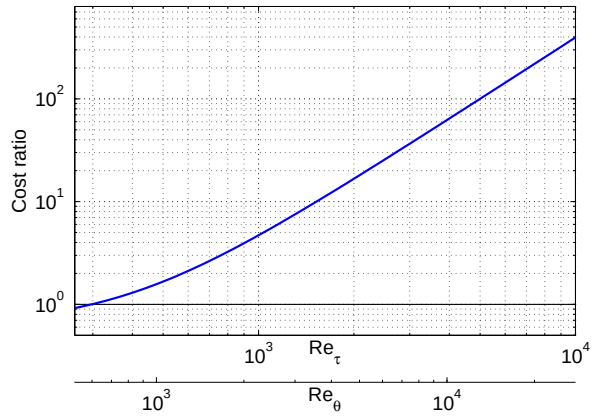

(b) The ratio of the total number of grid points required for LES divided by the number required for WMLES.

Fig. 1 The estimated number of grid points required to resolve a patch of area δ^2 of a boundary layer of thickness δ using both traditional LES and wall-modeled LES (WMLES). The cost for DES97 is given as a range, assuming a wall-parallel grid-spacing $\Delta x = \Delta z \gtrsim 0.5\delta$.

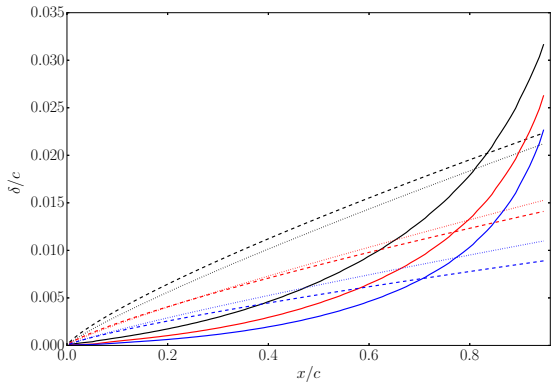

(a) Streamwise growth of the boundary layer thickness δ normalized by the chord c (solid lines), compared to the flat-plate correlations $\delta/x = 0.37{\cdot}10^{-1/5}$ (dashed; by Chapman, 1979) and $\delta/x = 0.16{\cdot}10^{-1/7}$ (dotted; by Choi & Moin, 2012).

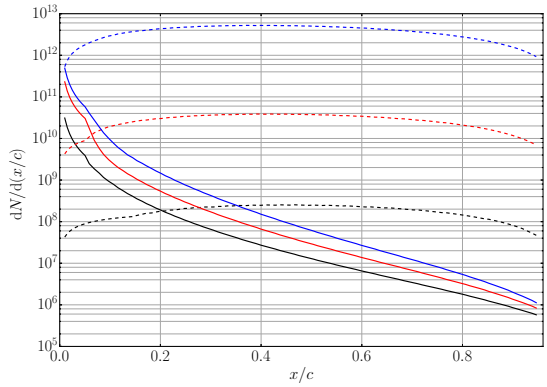

(b) Density of grid points required to resolve the outer layer using either LES or WMLES (solid lines; $y/\delta > 0.2$) and required for the inner layer using LES (dashed lines; $y/\delta < 0.2$) for a spanwise width of $0.1c$.

Fig. 2 The estimated grid-requirements for LES of the flow along the upper surface on a NACA0012 airfoil at 2.5° angle-of-attack at different chord Reynolds numbers of $Re_c = 10^6$ (black), 10^7 (red) and 10^8 (blue).

stress-modeled LES is only grid-independent if the grid is sufficiently fine for *both* of these solutions. We postpone a full discussion until section 3.2, and simply use the resulting recommendation of $(\Delta x/\delta, \Delta y_w/\delta, \Delta z/\delta) \approx (0.08, 0.02, 0.05)$, with linear variation up to $y/\delta = 0.2$ This estimate is also shown in Fig. 1(a), and is clearly independent of Re_τ.

The ratio of the total number of grid points in LES compared to WMLES is shown in Fig. 1(b). At $Re_\tau \lesssim 600$, going from LES to WMLES will save at most 50% of the grid points; while a significant saving, the reduced confidence in the results is hardly worth it. Therefore, wall-modeled LES is only meaningful at sufficiently high Reynolds numbers, for which the boundary layer has a clear multi-scale character with a separation of scales between the inner and outer layers that justifies the underlying philosophy of treating them differently.

Having compared WMLES to LES (the next higher fidelity), let us also compare to DES97 (the next lower fidelity) for this simple example. Since there is no upper limit on the wall-parallel grid-spacings Δx and Δz in DES97 for a boundary layer, we actually cannot really estimate the cost in this case. Instead, these grid-spacings would depend on the larger geometry, just like in RANS. Nevertheless, for the sake of comparison, the cost of DES97 is included in Fig. 1(a) for the range of wall-parallel grid-spacings $\Delta x/\delta = \Delta z/\delta \gtrsim 0.5$. WMLES incurs a cost 10-100 times higher than DES97, depending on the geometry.

We conclude this section by estimating the grid for a more realistic example: a NACA0012 airfoil at 2.5° angle-

	$Re_c = 10^6$	$Re_c = 10^7$	$Re_c = 10^8$	exponent in $\sim Re_c^\alpha$
Inner layer ($y/\delta < 0.2$)	1.7e8 (1.1e8)	2.6e10 (1.4e10)	3.5e12 (1.6e12)	2.16 (2.08)
Outer layer ($y/\delta > 0.2$)	6.3e8 (4.0e8)	4.3e9 (2.3e9)	9.2e9 (4.2e9)	0.58 (0.51)
Re_τ at trailing edge	3000	25000	200000	

Table 1 Total number of grid points required for LES on the upper surface of a NACA0012 airfoil at 2.5° angle-of-attack at different chord Reynolds numbers Re_c. Given for two different spanwise domain sizes of one-tenth of the chord (first number) and twice the boundary layer thickness at the trailing edge (second number, in parentheses). The last column gives the exponent α in the approximate scaling $\sim Re_c^\alpha$.

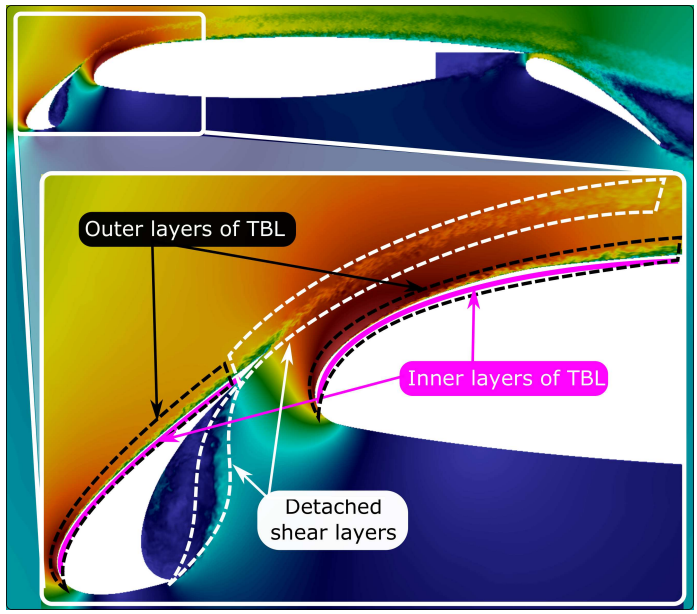

Fig. 3 Instantaneous flow field around a MD 30P/30N high-lift airfoil with deployed slat and flap, highlighting the differences between traditional LES (which resolves the energetic eddies everywhere), wall-modeled LES (which models the energetic eddies only in the inner part of the boundary layers, and resolves them in the outer layers and in all detached shear layers), and DES97 (which models the complete boundary layers, and resolves only the detached shear layers).

of-attack. The flowfield is computed by RANS using the Spalart-Allmaras model at three different Reynolds numbers, assuming a fully turbulent boundary layer everywhere (consistent with a swept wing, see Spalart *et al.*, 1997). The boundary layer thickness at each location along the upper surface is then extracted and shown in Fig. 2(a) along with some standard estimates for flat plates. The boundary layer growth is quite different on the airfoil compared with the flat plate, with lower growth in the accelerating region and faster growth farther downstream. The number of grid points required for a segment of length dx is shown in Fig. 2(b). For the outer layer, the required grid-density (for fixed span) is proportional to $1/\delta(x)^2$ (since Δx and Δz scale with δ), and thus most grid points for the outer layer are needed near the leading edge of the airfoil. For the inner layer, the scaling is more complex and involves the local skin friction. The total (integrated along x) costs are given in Table 1. The numbers are comparable to the estimate by Spalart *et al.* (1997) but much higher than those of Choi & Moin (2012), by about a factor of 100 for the inner layer and a factor ranging from 40 (highest Re_c) to 700 (lowest Re_c). This is caused by the streamwise variation of δ in Fig. 2(a), specifically the first third of the airfoil for which the flat-plate assumption underestimates the grid-requirements quite substantially.

2.2. Distinction between LES, WMLES and DES

It is important to realize that wall-modeled LES and DES97 (the original version of DES, as conceived by Spalart *et al.*, 1997) are very different methods in terms of philosophy, computational cost, and potential accuracy. Consider the visualization in Fig. 3, which shows an instantaneous snapshot of the flow over a multi-element airfoil. Different regions of the flow have been marked in the figure: (a) the detached shear layers; (b) the outer part of the boundary layers; and (c) the inner part of the boundary layers. The energetic and dynamically important motions are resolved in all of these regions in traditional LES (appropriately termed "quasi-DNS" by some authors). The important distinction is that wall-modeled LES resolves the energetic motions in regions (a) and (b), while DES97 only resolves those in region (a).

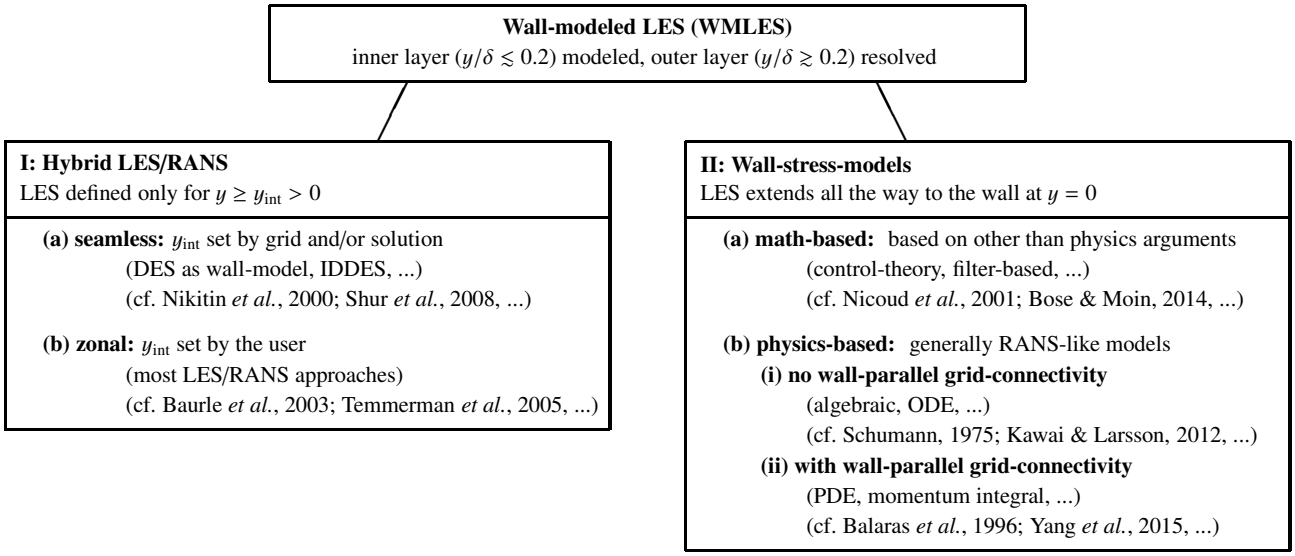

Fig. 4 Classification of wall-modeled LES (WMLES) approaches, with some representative citations given for each approach.

This distinction is very important: it means that WMLES has the potential to be significantly more accurate than DES97 in non-equilibrium flows. In RANS and DES97, the accuracy of the turbulence model in the non-equilibrium (e.g., adverse pressure-gradient) boundary layer is likely to determine the accuracy of the overall simulation (for flow separation over a smooth surface, or a similar flow). In WMLES, however, 80% of the boundary layer is treated by LES, which is perfectly capable of capturing any non-equilibrium effects. Provided that the outer layer LES is accurate, the wall-model is fed accurate instantaneous information, regardless of whether the wall-model itself accounts for non-equilibrium effects or not. Therefore, it is plausible that WMLES could still be accurate for a non-equilibrium flow, *even if the wall-model itself assumes equilibrium*. The caveat here is that it is also possible that an inaccurate wall-model could have affected the outer layer LES in the upstream region, thus making the outer layer LES inaccurate; we discuss this caveat in section 4.4. Nevertheless, even with this caveat, this overall reasoning is a very important point that is sometimes lost in parts of the wall-modeling community. A different line of reasoning that leads to the same place is the following: the turbulent time-scale is much faster in the inner layer than in the outer, and thus it is plausible that the inner layer may respond in an almost quasi-equilibrium manner to any outer flow time-history. More on this important point in section 3.4.

2.3. Taxonomy of WMLES methods

The term "wall-modeled LES" or "WMLES" is used in this paper to include all types of methods where the energetic scales of turbulence are modeled in the inner layer but resolved in the outer layer. Beyond this definition, there are different ways to categorize or classify different types of WMLES approaches (cf. Piomelli & Balaras, 2002; Spalart, 2009, for some different classifications).

The classification used here, sketched in Fig. 4, is based on how the resolved and modeled regions are coupled with each other. In this view, the most important distinction is whether the LES region is formally defined as extending all the way to the wall (at $y = 0$) or not. In hybrid LES/RANS methods, the LES region exists only above some "interface" y_{int} (which may be defined implicitly, but nevertheless exists), and the evolution equations change to a RANS-character below y_{int}. In contrast, the LES equations extend all the way down to the wall in the second major class of methods, which implies that they then require the wall shear stress τ_w as a boundary condition; a wall-model is then solved over a layer of thickness h_{wm} to estimate this wall-stress τ_w.

The distinction between hybrid LES/RANS and wall-stress-models is very subtle but nevertheless important. In the latter, while a RANS model is likely used to estimate the wall-stress, the coupling between the LES and RANS models is rather weak: the LES feeds velocity information to the (RANS) wall-model at $y = h_{\text{wm}}$, and the wall-model feeds wall shear stress τ_w to the LES at $y = 0$. Apart from these, no other information is exchanged. Notably, while the LES could impart flow structures onto the wall-model, the ability of "flow structures" in the wall-model to enter the LES region is

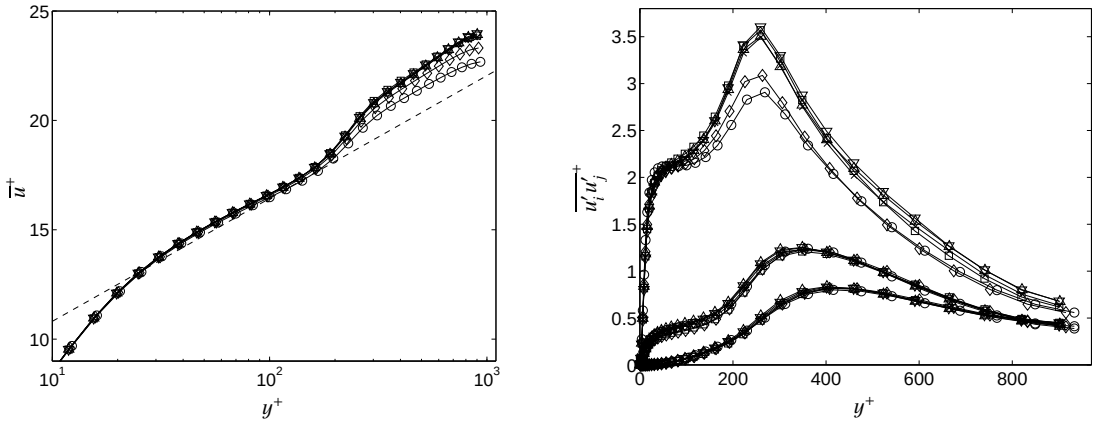

(a) Mean velocity $\overline{u}^+$.

(b) Normal Reynolds stresses $\overline{u'u'}^+$ (top), $\overline{w'w'}^+$ (middle) and $\overline{v'v'}^+$ (bottom).

Fig. 5 Grid-convergence in hybrid LES/RANS of channel flow with fixed interface height $y_{\text{int}}/\delta = 0.15$ during grid-refinement of $\Delta x/\delta$ from 0.25 (circles) to 0.047 (triangles). The spanwise resolution was fixed at $\Delta z/\delta = 0.031$. Taken from Larsson (2006).

limited. Perhaps more importantly, the formal definition of the LES region all the way to the wall implies that the LES and the wall-model actually overlap for a distance of h_{wm}. As will be discussed in section 3.2, this overlap can be used to achieve grid-independent results.

2.3.1. Hybrid LES/RANS methods There have been many proposed versions of hybrid LES/RANS methods over the years, some using the same turbulence model in both regions (e.g., DES in WMLES mode; cf. Nikitin *et al.*, 2000), others using different models in the two regions (among many others, cf. Baurle *et al.*, 2003; Davidson & Peng, 2003; Temmerman *et al.*, 2005). The classification of different hybrid LES/RANS methods is non-unique; one could easily classify into zero-, one-, and two-equation models instead, for example. The classification used here is driven by whether one can reach a grid-independent solution or not.

The energetic eddies in the log-layer are of a size roughly proportional to the wall-distance. Since they are strongly damped in the RANS region, this means that the smallest resolved LES eddies will have a size proportional to the interface height y_{int}. Therefore, methods for which one can maintain a fixed y_{int} during grid-refinement are capable of reaching a grid-converged state; we term these "zonal" methods here (note that Piomelli, 2008, and many others use the term "zonal" in a different sense). An example of grid-convergence for such a method is shown in Fig. 5. Note that, for this particular case, the mean velocity profile actually becomes *less* accurate during grid-refinement. In other situations, the opposite may be true. The larger implication is that hybrid LES/RANS may require quite fine grids in order to be grid-converged. If not grid-converged, then the results (by definition) depend on the numerical method, and any conclusions arrived at may be code-specific.

The other type of hybrid LES/RANS methods has an interface location y_{int} that depends on the grid and/or the solution, in a way that it cannot be set independently by the user. We term these "seamless", with the most famous example being DES when used in a wall-modeling mode (Nikitin *et al.*, 2000). The main advantage of seamless methods is how they can be used on a range of applications and grids without any user-driven modifications. This is a real strength in applied engineering situations. The downside, of course, is that it is very difficult (or perhaps impossible?) to demonstrate grid-independence, at least in the sense meant here.

Both "seamless" and "zonal" hybrid LES/RANS methods suffer from some degree of problem in maintaining the correct mean velocity profile around the interface. Most often, the mean velocity $\overline{u}^+(y^+)$ in the LES region ends up above the log-law, and thus this is called the "log-layer mismatch". Multiple studies have reported improvements that can remove the log-layer mismatch, through either the addition of small-scale forcing or by tailoring the blending function between the RANS and LES eddy-viscosities.

Small-scale forcing has been used in quite a few studies (cf. Piomelli *et al.*, 2003; Davidson & Dahlström, 2005; Davidson & Billson, 2006; Keating & Piomelli, 2006), with generally successful results in the sense of a reduced log-layer mismatch. The addition of small-scale forcing can be justified quite rigorously based on the filtered/averaged Navier-Stokes equations (Germano, 2004; Rajamani & Kim, 2010). The caveat, however, is that the results depend quite strongly on the forcing amplitude: this can be seen in Fig. 6, which shows how the log-layer mismatch is essentially a

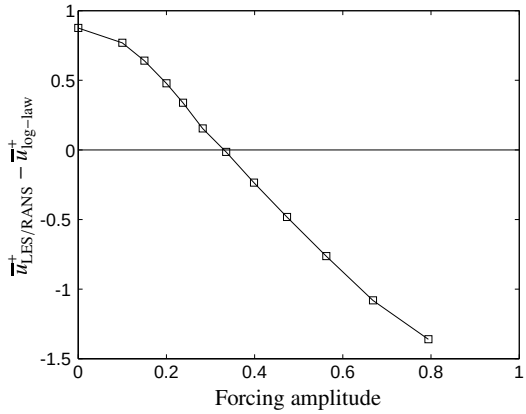

Fig. 6 Log-layer mismatch in hybrid LES/RANS and its dependence on the amplitude of small-scale forcing. Taken from Larsson *et al.* (2006).

linear function of the forcing amplitude (for this particular case, code, modeling approach, grid, etc). Clearly one can effectively remove the log-layer mismatch by picking the right forcing amplitude, but since there is no real theory or predictive way of doing this, the idea of using small-scale forcing in hybrid LES/RANS has a robustness problem. In fact, Keating & Piomelli (2006) and Larsson *et al.* (2006) both resorted to feedback-control algorithms in order to set the forcing amplitude.

The other major approach to reducing the log-layer mismatch has been to adjust the blending function between the LES and RANS eddy-viscosities. Choi *et al.* (2009) found the best results when aiming for an interface near the boundary between the log-layer and the outer layer. Shur *et al.* (2008) used a blending function that caused a more abrupt changeover, arguing that this promotes instabilities that more rapidly lead to resolved LES turbulence. Given the dependence of the log-layer mismatch on the grid illustrated in Fig. 5, however, the question remains as to how robust these methods are to different grid resolutions and different numerical methods (which add method-specific numerical errors). In fact, when testing with different Δx values, Shur *et al.* (2008) did find differences in the mean velocity profile, including a non-zero log-layer mismatch for $\Delta x = 4\Delta z$. While one could argue that such a grid should not be used, it would be nice to see evidence of grid-independence for different types of numerical methods for the promising ideas of Shur *et al.* (2008).

To summarize, the major drawback of the hybrid LES/RANS methods clearly is their "artificial buffer layer" with the associated log-layer mismatch and the artificial physical structures that survive some distance into the LES region (cf. Piomelli *et al.*, 2003). Countering this drawback is the major advantage of how at least some of these methods can function in both LES/RANS and in pure RANS mode, depending on the state of the flow and the grid. This can be very valuable in applied situations.

2.3.2. Wall-stress-models Almost all wall-stress-models are based on the physical principle of momentum conservation in a nearly parallel shear flow. The whole point of wall-modeling is to avoid resolving any turbulence in the inner layer, and thus the wall-model equations must necessarily be thought of as either low-pass filtered in the wall-parallel directions or ensemble-averaged. In either case, the filtered momentum conservation equation in the (on average) streamwise direction is

$$\frac{\partial u}{\partial t} + \frac{\partial u\, u_j}{\partial x_j} + \frac{1}{\rho}\frac{\partial p}{\partial x} = \frac{\partial}{\partial y}\left[(\nu + \nu_{t,\mathrm{wm}})\frac{\partial u}{\partial y}\right], \tag{1}$$

where we have assumed the special case of uniform-density flow aligned (on average) with the $x = x_1$ direction. In addition to the parallel-flow assumption, most wall-stress-models assume that the eddy-viscosity in the wall-model $\nu_{t,\mathrm{wm}}$ is given by a zero-equation mixing-length model like

$$\nu_{t,\mathrm{wm}} = \kappa u_\tau y \left[1 - \exp\left(-y^+/A^+\right)\right]^2 . \tag{2}$$

The most common wall-stress-model is the equilibrium model, in which the convection and the pressure-gradient are assumed to balance exactly; thus the left-hand-side of Eqn. (1) is assumed to be zero. The resulting ODE has the solution $u^+ \approx y^+$ for $y^+ \lesssim 5$ and $u^+ \approx \ln(y^+)/\kappa + B$ for $y^+ \gtrsim 30$, as is well known. In practice, equilibrium models can be implemented either by algebraically solving the log-law for the friction velocity u_τ, or by numerically solving

the ODE directly. The slight advantage of the latter is that it produces the right wall-stress even if the grid locally approaches traditional LES resolution with resolved viscous and buffer layers. The more significant advantage of the algebraic implementation is, of course, that it is considerably cheaper. In practice, the only reason to solve the equilibrium ODE numerically is the ability to account for other physics-effects, e.g., in the case of strongly non-adiabatic compressible flow. We note that ODE-based wall-models have also been considered in the RANS literature (e.g. Craft *et al.*, 2004) to improve the prediction of the wall shear stress by solving an ODE in the wall-normal direction inside an inner layer sufficiently close to the wall.

The first one to actually solve the momentum equation (1) as a wall-stress-model, with all terms retained (i.e., solving the full boundary layer PDEs), was Balaras *et al.* (1996). This removes the assumption of a perfect balance between convection and the pressure-gradient, which should enable the capturing of at least some non-equilibrium effects. Others have followed in the footsteps of Balaras *et al.* (1996), proposing different modifications to their original concept. Cabot & Moin (1999) pointed out that the eddy-viscosity model coefficient κ in Eqn. (2) should be reduced when solving the full momentum equation (1), since the convection terms then carry some shear stress. Wang & Moin (2002) introduced a dynamic procedure for κ, which Kawai & Larsson (2013) later corrected to maintain physical consistency at larger Reynolds numbers. Park & Moin (2014) then proposed a modified correction for cases where spatial averaging can be performed (most notably, spanwise periodic cases).

The major disadvantage of solving the boundary layer PDEs is the requirement of a separate near-wall grid. To solve PDEs, this grid must have full connectivity in all coordinate directions, with similar grid-quality requirements as a normal RANS grid. The generation of this separate grid was not a problem in the academic studies mentioned above, but could clearly present significant problems in more realistic and complex geometries. Primarily for this reason, there exists a clear opportunity for innovative wall-stress-models that do not assume equilibrium and yet require at most a system of ODEs in the wall-normal direction to solve. Some such models are discussed in section 3.4, along with the consistency requirements that they must satisfy.

The wall-stress-models discussed up to this point have all been physics-based, i.e., derived based on physical principles and arguments. A very different approach to the problem was taken by Nicoud *et al.* (2001), who viewed the problem in a purely mathematical sense. By the late 1990s, it had become clear that the LES was always underresolved in the first grid points next to the wall when used in combination with a wall-stress-model. Given that fact, one could plausibly conclude that physics-based modeling would never be sufficient – even a perfect wall-stress-model would suffer from errors in the underresolved LES. This line of thinking led to the innovative paper by Nicoud *et al.* (2001), which viewed the instantaneous wall-stress field as a control input, and used control theory to find the wall-stresses that caused the LES mean velocity to most closely follow the log-law. This approach was further developed by Templeton *et al.* (2006, 2008). A different approach that also viewed the problem in a purely mathematical sense is the work of Bose & Moin (2014), who viewed the wall-modeling problem in terms of filtering without direct reference to the near-wall physics. They argued that the filtered velocity at a wall should have a finite value (i.e., a slip-velocity), and proposed a method for estimating this slip-velocity given an instantaneous LES solution and grid. An important future development for this model will be to quantify the effects of the strong connection between the filter-width (both size and anisotropy) in the LES and the implied wall-model on the accuracy of the results (i.e., do the results change for different $\Delta x/\Delta z$ ratios in the grid and/or filter?). As a side-point, the Bose & Moin (2014) approach does not really fit the present taxonomy in Fig. 4: it does define the LES all the way to the wall, but it does not estimate the wall-stress directly.

The remainder of the paper is focused on physics-based wall-stress-models, specifically on the progress during the last decade.

3. Wall-stress modeling: implementation and recent progress on key issues

The principle of wall-stress-modeled LES is sketched in Fig. 7. The problem can be stated in the following way: given an instantaneous velocity u_i at height $y = h_{\mathrm{wm}}$ above the wall, estimate the instantaneous wall shear stress vector $\tau_{w,i}$. If one is solving an energy equation at the LES level, this is augmented by the estimation of the wall heat flux q_w using the temperature T at height $y = h_{\mathrm{wm}}$ as input. And, one could easily add additional input quantities, for example the velocity gradient tensor $\partial_j u_i$, the pressure-gradient $\partial_i p$, and other quantities available in the LES. The implementation in a complex geometry when the LES grid is unstructured is sketched in Fig. 8.

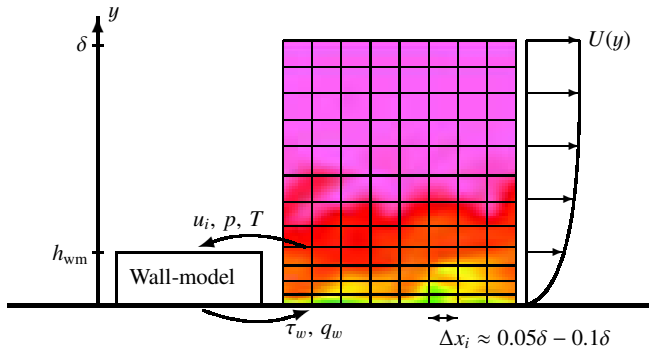

Fig. 7 The principle of wall-stress-modeled LES if the wall-model is decoupled from the LES grid. Instantaneous snapshot of a boundary layer with overlaid LES grid, where the grid-spacing Δx_i in all directions is determined solely by the boundary layer thickness δ. The wall-model models the flow in a layer of thickness h_{wm}; it is fed instantaneous velocity and temperature information from the LES, and returns the instantaneous wall stress and heat flux to the LES, which then uses these as the wall boundary condition. The wall-model thickness h_{wm} is chosen to fall within the log-layer.

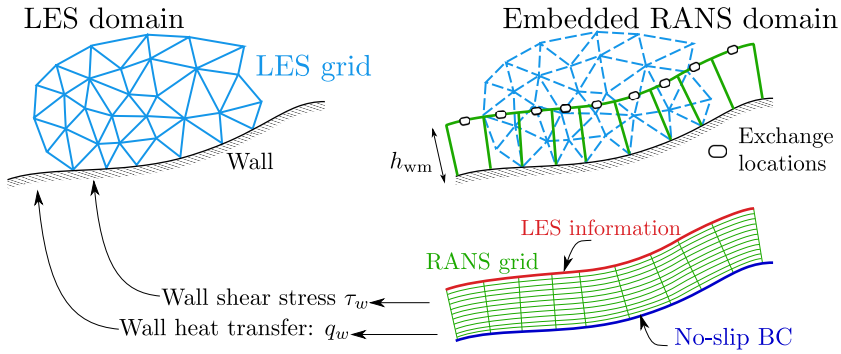

Fig. 8 Implementation of wall-stress-modeled LES where the wall-model is decoupled from the LES grid in complex geometries. The wall-modeled thickness h_{wm} is specified independently from the LES grid, which necessitates interpolation from the LES grid to the top of the wall-modeled layer. Taken from Bodart & Larsson (2011).

3.1. Implementation – numerical integration of ODE-based models

The implementation of an algebraic wall-stress-model is often trivial, but it is worth spending some time describing the implementation of an ODE-based wall-stress-model. We consider the case of implementing an equilibrium-model for compressible flow, for which the simplified momentum and total energy equations are

$$\frac{d}{dy}\left[(\mu+\mu_{t,\mathrm{wm}})\frac{dU}{dy}\right]=0\,, \tag{3}$$

$$\frac{d}{dy}\left[c_p\left(\frac{\mu}{Pr}+\frac{\mu_{t,\mathrm{wm}}}{Pr_{t,\mathrm{wm}}}\right)\frac{dT}{dy}\right]=-\frac{d}{dy}\left[(\mu+\mu_{t,\mathrm{wm}})\,U\frac{dU}{dy}\right]\,, \tag{4}$$

and the wall-model eddy-viscosity is taken as

$$\mu_{t,\mathrm{wm}}=\kappa\rho\sqrt{\frac{\tau_w}{\rho}}\,y\left[1-\exp\left(-y^+/A^+\right)\right]^2\,. \tag{5}$$

Note that the velocity scale for non-uniform density is $\sqrt{\tau_w/\rho}$. We take the common values $\kappa=0.41$, $A^+=17$ and $Pr_{t,\mathrm{wm}}=0.9$.

These equations are to be solved over the region $0\le y\le h_{\mathrm{wm}}$. At the top boundary, U is set equal to the magnitude of the wall-parallel velocity in the LES, while T is simply taken directly from the LES. At the lower boundary, the no-slip condition is applied together with the appropriate thermal boundary condition (specified temperature or heat flux).

It is worth pointing out that Eqn. (4) is derived from the conservation of total energy, and therefore this equation does contain the effect of viscous heating. Specifically, the term involving the velocity U is the sum of the viscous heating $(\mu+\mu_{t,\mathrm{wm}})(dU/dy)^2$ (which includes heating by turbulence dissipation, since the assumption of equilibrium implies that turbulence production $\approx$ dissipation) and the work done by viscous forces and turbulence $Ud((\mu+\mu_{t,\mathrm{wm}})dU/dy)/dy$.

Eqns. (3) and (4) are in divergence-form and are thus most naturally solved using a 1D finite-volume method. The 1D finite-volume grid can be stretched quite substantially (each cell can be 10-20% larger than its next neighbor). In our own implementations, we have used second-order accurate interpolation and differentiation at the cell faces, and then solved the coupled equations using the tri-driagonal matrix or Thomas algorithm (TDMA) applied in a segregated manner (alternating TDMA sweeps of the momentum and energy equations, with updated eddy-viscosity $\mu_{t,\mathrm{wm}}$ in between). The convergence is easiest measured by the change in τ_w and q_w between successive iterations, since these are the only output quantities from the wall-model.

The wall-stress τ_w from the wall-model (3)-(5) is the magnitude of the wall-stress vector parallel to the wall. The final step is to construct the full wall-stress vector $\tau_{w,i}$ by assuming that it is perfectly aligned with the velocity parallel to the wall, and by using a simple linear approximation for the wall-normal velocity (for the wall-normal stress).

3.2. The log-layer mismatch – root cause and a physics-based solution

One of the most persistent errors in wall-modeled LES is the "log-layer mismatch", where the mean velocity profile in viscous units is shifted upwards (positive mismatch, $\overline{u}^+$ above the log-law) or downwards (negative mismatch, $\overline{u}^+$ below the log-law). Since the skin friction coefficient $c_f = 2\tau_w/(\rho_\infty U_\infty^2) \propto U_\infty^{+\,-2}$, the log-layer mismatch error has a direct effect on the predicted skin friction. Accurate prediction of the skin friction is important not only for drag predictions, but also in predictions of boundary layer separation, where the cumulative loss of near-wall momentum in the upstream boundary layer determines the point of separation.

Experience has shown that the straightforward application of most wall-modeled LES approaches in both categories in Fig. 4 (i.e., both hybrid LES/RANS and wall-stress-models) leads to a log-layer mismatch. Importantly, the log-layer mismatch depends both on the actual wall-model *and* on details of the LES method itself (numerics, grid, subgrid model, etc). A positive log-layer mismatch has been found for almost all versions of hybrid LES/RANS (cf. Nikitin *et al.*, 2000; Piomelli *et al.*, 2003; Larsson *et al.*, 2006; Hamba, 2009; Chen *et al.*, 2012). For wall-stress-models, some studies find a positive mismatch (cf. Piomelli *et al.*, 1989; Kawai & Larsson, 2012) while others find a negative mismatch (cf. Cabot & Moin, 1999; Nicoud *et al.*, 2001; Lee *et al.*, 2013; Bose & Moin, 2014). Interestingly, the studies with a negative mismatch has generally been for incompressible flow solved using a staggered grid, whereas most results with codes using a colocated grid and/or some degree of numerical dissipation have produced a positive mismatch. The main point of this observation is, of course, that the log-layer mismatch is code-dependent, more specifically dependent on the numerics and modeling in the LES itself.

For the case of wall-stress-modeled LES, there does exist a robust solution to the log-layer mismatch problem. The solution is best understood in terms of grid-convergence, specifically by framing the wall-modeled LES problem in the following way. Assuming that we know the local boundary layer thickness δ, from a physics point-of-view we know that the "ideal" thickness of the wall-modeled layer is $h_{\mathrm{wm}} \approx 0.2\delta$ (i.e., the bottom of the outer layer). Thus we should specify h_{wm} without any reference to the LES grid. Having made this specification, we should now seek an LES grid that is sufficiently fine to yield grid-converged results. As it turns out, once h_{wm} is specified and held fixed, the LES solution displays classical grid-convergence behavior, with grid-converged results once the grid-spacing is some fraction (the exact value of which depends on the numerical method) of h_{wm}. Importantly, the converged results have zero log-layer mismatch. The remainder of this section lays out the details of this approach and why it works, following Kawai & Larsson (2012).

Consider a wall-stress-modeled LES where the wall-model takes as input the instantaneous LES solution at some height $y = h_{\mathrm{wm}}$. The most natural choice, and the choice made historically, is to take the LES solution from the first off-wall grid point as input to the wall-model (i.e., to choose $h_{\mathrm{wm}} = \Delta y$ or $\Delta y/2$ depending on grid-arrangement). The problem, however, is that the LES is inevitably plagued by numerical and subgrid-modeling errors in the first few grid points off the wall, for the following reasons. The size of the energetic and stress-carrying motions in the log-layer is roughly proportional to the wall-distance y, and thus the length scale of the stress-carrying motions in each direction i can be written as $L_i = C_i y$, where C_i is a constant that is different in each direction. To resolve eddies of size L_i numerically, a grid-spacing of $\Delta x_i \lesssim L_i/N$ is needed, where N is the number of grid points per integral scale L_i. The exact value of N depends on the numerical method, with smaller values expected for higher-accuracy methods. Therefore, the stress-carrying motions are properly resolved at height y only if

$$\Delta x_i \lesssim \frac{C_i}{N}\, y \;, \quad i = 1, 2, 3\,. \tag{6}$$

The numerical Nyquist criterion implies that $N \gtrsim 2$ (i.e., at least 2 points are needed per wavelength). Kinematic damping

of turbulent eddies by the wall makes $C_2 \lesssim 2$ a reasonable upper bound. Therefore, C_2/N is almost certainly less than 1, which means that the criterion (6) is violated in the first LES grid-point, regardless of numerical accuracy in the LES. As a direct consequence, the LES is necessarily inaccurate in the first grid-point, and thus the wall-model is necessarily fed inaccurate input from the LES *whenever we define the wall-model to start at the first LES grid-point*.

A crucial implication of the reasoning above is that the error is not due to the wall-model, and thus even a "perfect" wall-model in one numerical code would suffer from a log-layer mismatch if implemented in a different numerical code!

The solution to the problem is very simple, and stems directly from criterion (6) and the realization that the wall-model equations (3)-(5) are valid for *any* interval between the wall and the bottom of the outer part of the boundary layer. Specifically, for a fixed h_{wm}, the LES will be grid-converged if and only if

$$\Delta x \lesssim \frac{C_1}{N} h_{\text{wm}} \ , \quad \Delta y \lesssim \frac{C_2}{N} h_{\text{wm}} \ , \quad \Delta z \lesssim \frac{C_3}{N} h_{\text{wm}} \ . \tag{7}$$

We can satisfy the criteria (7) in the wall-parallel directions by simple grid-refinement of Δx and Δz. The criterion on Δy, however, can only be satisfied by decoupling the LES grid (i.e., Δy) from the thickness of the wall-modeled layer (i.e., the modeling choice h_{wm}) – in other words, by abandoning the established practice of applying the wall-model between the first off-wall grid point and the wall. The overall reasoning is that the wall-model can only function properly if fed accurate information from the LES, which in turn implies that the LES must be well resolved at the point h_{wm} (the modeling choice) where information is fed to the wall-model.

An example of this reasoning and the resulting approach is shown in Fig. 9. By refining Δy while keeping the modeling choice h_{wm} fixed, there is clearly a convergence process of the LES results. The fact that we can reach a grid-converged state, i.e., a state where the numerical and modeling errors *in the LES* are negligible, is the main point of the approach by Kawai & Larsson (2012). The fact that the mean velocity in this example actually converges to the expected log-law is then a conclusive proof that the wall-model is accurate for this flow. This implies two things: (i) that this approach is a robust solution to the log-layer mismatch problem; and (ii) that this type of framework that can remove errors in the LES should be used when assessing wall-models on other types of flows – the effect of the wall-model must be isolated before any meaningful assessment can be made (which is unfortunately sometimes bypassed in the wall-modeling community).

For the particular numerical method used in this example (sixth-order accurate compact differencing scheme), essentially converged results are obtained for $\Delta y \lesssim 0.33\, h_{\text{wm}}$. The complete grid-convergence study suggests that $\Delta x \approx \Delta z \lesssim 0.8\, h_{\text{wm}}$ is required/sufficient for grid-converged results for the particular numerical method used by Kawai & Larsson (2012). This reasoning was later confirmed in the independent study by Lee *et al.* (2013), who found grid-converged results in their channel flow calculations (using a very different numerical method) for $\Delta x \lesssim 0.6\, h_{\text{wm}}$, $\Delta y \lesssim 0.3\, h_{\text{wm}}$, and $\Delta z \lesssim 0.4\, h_{\text{wm}}$. Every code will have its own exact requirements, but the larger reasoning is general.

Having described the Kawai & Larsson (2012) framework, it is appropriate to mention the work of Brasseur & Wei (2010), who conducted a comprehensive analysis of what errors in the LES (i.e., not in the wall-model) that lead to a mean velocity gradient that is different from the log-law. They identified the grid-dependence in wall-modeled LES, both the dependence on grid-spacing and grid-anisotropy. While they did not decouple the LES grid from the thickness of the wall-modeled layer, i.e., allow for $\Delta y \ll h_{\text{wm}}$, their theory of different errors could be used in the Kawai & Larsson (2012) framework to predict the required grid-spacings for a grid-converged solution.

Finally, we note the work of Wu & Meyers (2013), who addressed the log-layer mismatch problem in a different way. They similarly noted that the LES is inevitably erroneous near the wall, but solved this by deriving the value of the Smagorinsky constant (they used the Smagorinsky subgrid model) that would lead to a mean velocity profile that satisfies the log-law. This modified Smagorinsky constant, used only near the wall, was found to reduce the log-layer mismatch error from a typical 10-20% to only 5% in their numerical tests. An interesting future direction would be to combine their modified Smagorinsky constant with the framework for grid-converged WMLES, the idea being that it could possibly reduce the grid-requirements for reaching grid-convergence.

3.3. Transition to turbulence

Many important flows are sensitive to the laminar-to-turbulence transition process, including the flow over a cylinder or sphere around the drag crisis, the flow over an airfoil at high angles-of-attack, and the heat transfer around a hypersonic vehicle. Traditional LES approaches can predict the transition process rather accurately, since the instability waves and mechanisms important to the transition process are fully resolved on a grid suitable for traditional LES. Existing wall-modeled LES approaches, on the other hand, cannot predict transition: since the wall-model assumes fully developed

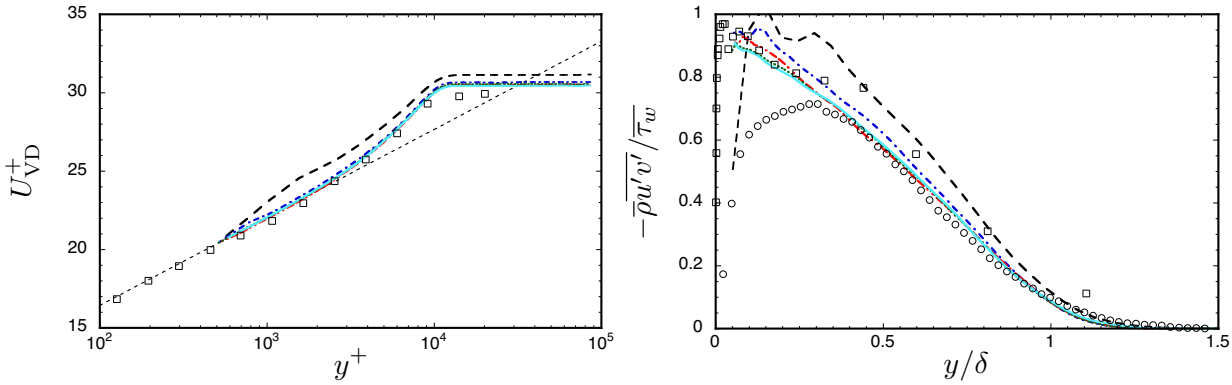

(a) Mean velocity (van Driest-transformed).

(b) Reynolds shear stress.

Fig. 9 Mean velocity (van Driest-transformed) and Reynolds shear stress obtained by LES with wall-stress-model for a supersonic flat-plate boundary layer at $Re_\delta = 6.1 \times 10^5$ ($Re_\theta = 5 \times 10^4$). The mean velocity (on left) is compared to the log-law $\ln(y^+)/0.41 + 5.2$ (thin dashed line, black) and incompressible experiments (squares, De Graaff & Eaton (2000)). The Reynolds shear stress (on right) is compared to corresponding experiments (circles, Souverein *et al.* (2010)) and incompressible experiments (squares, De Graaff & Eaton (2000)). The wall-modeled layer has a fixed thickness of $h_{\mathrm{wm}}/\delta = 0.055$, and the wall-parallel LES grid is fixed at $\Delta x/\delta = \Delta z/\delta = 0.042$. The wall-normal LES grid-spacing is varied as $\Delta y_w/h_{\mathrm{wm}}$ of 1.0 (dashed line, black), 0.50 (dashed-dotted line, blue), 0.33 (double-dashed double-dotted line, red), 0.25 (dotted line, green), 0.20 (solid line, cyan). Taken from Kawai & Larsson (2012).

turbulence, the wall-model predicts a high level of wall shear stress τ_w even in the laminar region, resulting in inaccurate boundary layer growth and dynamics. An example of this problem was the inability to predict the drag crisis in the flow around a cylinder by Catalano *et al.* (2003), where the wall-model predicted a turbulent boundary layer around the full cylinder, with the associated late separation and low coefficient of drag, regardless of the Reynolds number.

The problem of predicting transition with wall-modeled LES was studied and addressed by Bodart & Larsson (2012), who proposed a solution in which a flow sensor continuously estimates whether the local boundary layer is laminar or turbulent and then adjusts the wall-treatment accordingly. The underlying reasoning is that the instability waves in transition scale with outer units, i.e., they have wavelengths on the order of the boundary layer thickness δ rather than the viscous length scale. Therefore, a grid suitable for WMLES (following the criteria in section 3.2) is capable of accurately capturing the instability waves as well.

To estimate whether the boundary layer is laminar or turbulent, Bodart & Larsson (2012) made the observation that the turbulence kinetic energy in viscous units is consistently between 2.5 and 4.0 in the log-layer across a large range of Reynolds numbers. Since the top of the wall-modeled layer is in the log-layer, it makes sense to estimate the kinetic energy at that location. The turbulence kinetic energy at $y = h_{\mathrm{wm}}$ is estimated using a temporal low-pass filter with an exponential kernel, which allows a time-filtered value $\langle f \rangle$ of a quantity f to be approximately computed from the ODE (analogously to Meneveau *et al.*, 1996)

$$\frac{d\langle f\rangle(t)}{dt} = \frac{f(t) - \langle f\rangle(t)}{T(t)}, \tag{8}$$

where we take $T(t) = 1/\sqrt{S_{ij}S_{ij}}$ at $y = h_{\mathrm{wm}}$. This low-pass filter (or moving average) then allows for the estimation of the time-filtered wall density $\langle \rho_w \rangle(t)$, the time-filtered wall shear stress $\langle \tau_w \rangle(t)$, and the time-filtered turbulence kinetic energy $k(t) = \langle u_k u_k \rangle - \langle u_k \rangle^2$, taken at $y = h_{\mathrm{wm}}$. The proposed sensor is then (note that this is actually the square of the sensor defined in Bodart & Larsson, 2012)

$$s_w(t) = \frac{\langle \rho_w \rangle(t)\, k(t)}{\langle \tau_w \rangle(t)}, \tag{9}$$

which is defined at every point on the wall. This quantity is completely local and can be easily computed for any type of grid or geometry. The wall-model is used to estimate the wall stress τ_w (and possibly the wall heat flux q_w or the wall temperature T_w) at all points where $s_w(t) > s_{\mathrm{lim}}$, while the standard estimation of the shear stress assuming a linear velocity profile from the first off-wall grid-point is used where $s_w(t) < s_{\mathrm{lim}}$.

The results are rather insensitive to the threshold value s_{lim}, due to the fact that the turbulence kinetic energy in viscous units (which the sensor s_w estimates) is close to constant across different wall-distances and Reynolds numbers; Bodart & Larsson (2012) found $2.5 \lesssim s_w \lesssim 4.0$ for $20 \lesssim y^+ \lesssim 0.2\delta^+$ for several DNS channel flow simulations with

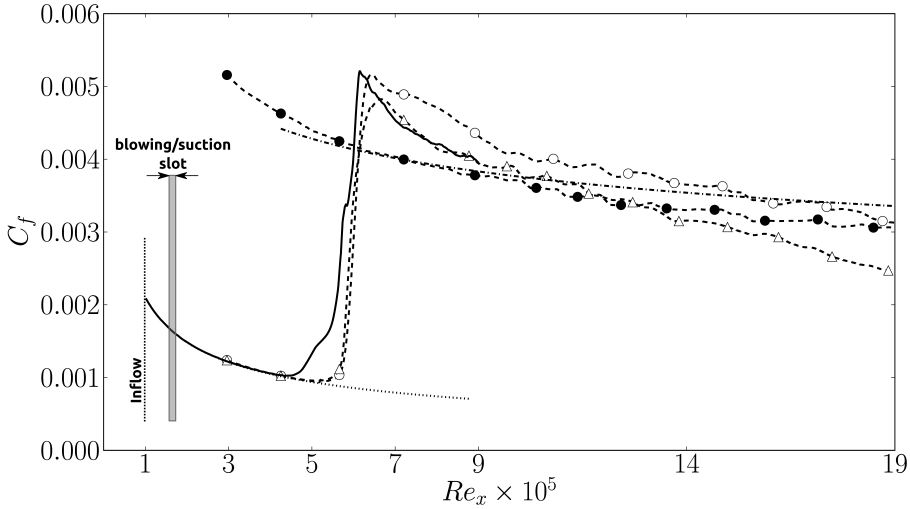

Fig. 10 Skin friction coefficient along a flat plate boundary layer undergoing transition, for WMLES with the transition-sensor (dashed line with open circles), standard WMLES without any sensor (dashed line with filled circles), and underresolved LES on the same grid but without any wall-model at all (dashed line with open triangles). The results are compared to the DNS of Sayadi *et al.* (2013) (solid line), the theoretical laminar result $c_f = 0.664 Re_x^{1/2}$ (lower dotted line), and the semi-analytical turbulent correlation $c_f = 0.455/[\log(0.06 Re_x)]^2$ (upper dash-dotted line). Taken from Bodart & Larsson (2012).

friction Reynolds numbers Re_τ ranging from 180 to 2000. A value of $s_{\text{lim}} = 0.25$ works well for the cases we have tried so far.

The approach is assessed by computing the transition induced by localized blowing and suction in the boundary layer over a flat plate. The blowing/suction triggers so-called H-type transition, where modes grow from infinitesimal levels in a linear manner before breakdown to turbulence. The main result, the skin friction coefficient c_f, is shown in Fig. 10.

The figure shows several things. The sensor is clearly required for this problem in order to avoid erroneously assuming a turbulent skin friction in the laminar region. With the sensor, the wall-modeled LES closely follows an underresolved LES (without any wall-model) up to the point of transition, exactly as designed. The effect of the coarse grid-resolution is to yield a much more abrupt transition than in DNS; however, the actual point of transition is very well predicted. Behind the transition location, the underresolved LES (without the wall-model) progressively starts underpredicting the skin friction, as the viscous length scale decreases and makes the LES increasingly poorly resolved. With the wall-model, the skin friction stays at the turbulent level.

One important caveat to these results is that while the instability waves are rather "large" in the wall-parallel directions, they do require a fine grid in the wall-normal direction in order to be accurately captured. For example, Park & Moin (2014) used the sensor-based WMLES technique to compute a transitional case, and found that they needed to refine the grid in the wall-normal direction in the transitional region. In an incompressible code, this can be achieved quite easily at little additional computational cost, but for compressible codes with explicit time-stepping such a refined wall-normal grid in the laminar region would induce a substantially reduced time step. In different transition scenarios where the disturbances come from the free-stream flow (e.g., "bypass transition") this may be much less problematic.

Finally, we note that the general idea of combining a wall-model with a sensor could be extended beyond the issue of laminar-to-turbulent transition. For example, sensors could be designed to deactivate the wall-model near or after flow separation.

3.4. Separating and separated flows

Flows where the boundary layer separates over a smooth surface are important in many engineering applications, and are known to be poorly predicted by many RANS methods. Therefore, there is great interest in finding a wall-modeled LES method which is robustly accurate for separating and separated flows.

3.4.1. Why the assumption of equilibrium in a wall-model is less restrictive than at first sight A common line of thinking in the wall-modeling community is that equilibrium models are necessarily erroneous and insufficient for non-equilibrium flows. There are, however, two main arguments that depart from this pessimistic view and justify the applicability of such models in non-equilibrium conditions.

First, 80% of the boundary layer in wall-modeled LES is resolved. A properly conducted WMLES should have

the same grid-resolution in the outer layer as a normal LES, and should therefore capture the non-equilibrium effects in the outer layer with the same accuracy as traditional LES. Moreover, the turbulence time-scale k/ε is approximately proportional to the wall-distance y in the inner layer, and thus much of the inner layer dynamics are much faster than any large-scale dynamics in the outer layer (which the LES would capture). As a consequence, it is wholly plausible that the inner layer should be close to equilibrium, even in a non-equilibrium flow.

Secondly, it is crucial to remember the physical nature of the convection and pressure-gradient terms in the momentum equation (1), specifically that the left-hand-side of Eqn. (1) is the sum of terms that may be individually very large but which should approximately balance each other above the viscous layer. For example, a strong adverse-pressure-gradient should lead to flow deceleration, and vice versa. More mathematically, above the viscous layer and in the limit of weak turbulence, Eqn. (1) should reduce to the so-called "Euler-s" equation along a streamline, which, after integration along the streamline, becomes the Bernoulli equation. This hypothesis was tested by Hickel *et al.* (2012) using well-resolved (traditional) LES data for two strongly separated flows, with the conclusion that the instantaneous convective terms were almost perfectly balanced by the instantaneous pressure-gradient above the viscous layer (say, $y^+ \gtrsim 30 - 50$).

Putting these aspects together, we have the following plausible picture: Even in a strongly non-equilibrium boundary layer, the left-hand-side of Eqn. (1) is approximately zero in the overlap (log-) layer due to the balance between convection and pressure-gradient (physically, due to the Bernoulli equation). This balance does not hold in the viscous layer, of course, but due to the time-scale argument the viscous layer is the most likely to be in quasi-equilibrium. Therefore, we must conclude that the assumption of an approximately zero left-hand-side in Eqn. (1) is potentially rather accurate, even in non-equilibrium situations – at the very least, we should allow for the possibility of this being a reasonably accurate approximation.

There is some evidence for this conjecture in the recent paper by Coleman *et al.* (2015), who extracted the mean velocity at $y^+ = 50$ (denoted by $\overline{u}^+(y^+ = 50)$) from a wide range of adverse and favorable pressure-gradient flows. Across the full range of variation in pressure-gradient (dp^+/dx^+ ranging from -0.02 to 0.02), the $\overline{u}^+(y^+ = 50)$ value varied from about 16 (favorable) to about 14 (adverse). Thus the effect of the pressure-gradient should be weak, which is consistent with the idea that the sum of convection and pressure-gradient should be small, regardless of how large the individual terms are.

There has been some recent *a posteriori* evidence in favor of this conjecture. Bermejo-Moreno *et al.* (2014) performed WMLES with an equilibrium wall-model of the interactions between oblique shock waves and turbulent boundary layers in a nearly square duct. Despite the significant pressure gradients that exist within the boundary layer in the region of interaction with the shock wave, a favorable comparison with experimental data was found for this incipiently separated flow, as shown in Fig. 11. The good agreement seen in the figure offers strong support for the overall reasoning in this section, specifically that equilibrium wall-models can be accurate even in strongly non-equilibrium flows, provided that the outer part of the boundary layer is well resolved.

3.4.2. Non-equilibrium ODE-based wall-models While the equilibrium assumption is much less restrictive than the conventional wisdom gives it credit for, there is no question that a good, physically consistent, non-equilibrium wall-model requiring at most the solution of ODEs would be extremely useful. Put a different way, while the results of Coleman *et al.* (2015) discussed above suggest that the influence of the pressure-gradient is weak, the results also clearly show that there *is* an influence of the pressure-gradient.

The search for a wall-model that goes beyond the equilibrium assumption without requiring the solution of a PDE goes back at least to the paper by Hoffmann & Benocci (1995). All such efforts have been based on the following two observations: (i) a physics-based wall-model must be based on the momentum equation, since momentum transfer is the key physical process in a boundary layer; and (ii) the pressure-gradient is close to constant across a nearly parallel shear flow, and can thus be imposed from the LES solution without requiring any wall-parallel derivative when solving the momentum equation.

A common approach in the literature has been to simply discard the convective terms (i.e., $\partial(uu_j)/\partial x_j$) while retaining the pressure-gradient term and, in some cases, the time-derivative term as well (Hoffmann & Benocci, 1995; Wang & Moin, 2002; Catalano *et al.*, 2003; Duprat *et al.*, 2011; Chen *et al.*, 2014). This is physically inconsistent, following the reasoning and evidence in section 3.4.1 about how convection and pressure-gradient essentially balance each other outside of the viscous layer. In a similar vein, including the time-derivative term but discarding the convective term is also inconsistent, since it violates the physical fact that fluid accelerations are Lagrangian in nature. Therefore, we must conclude that the only physically consistent approach is to either retain or neglect all left-hand-side terms in Eqn. (1) together. In addition to the theoretical reasoning above, there is also evidence in the literature supporting this conclusion:

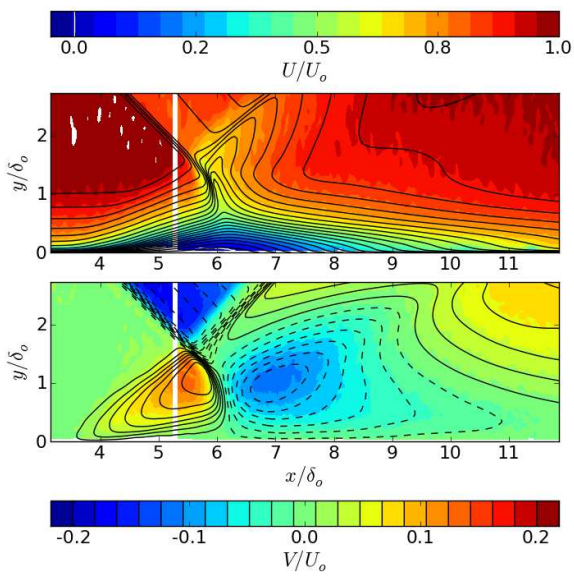

(a) Mean streamwise (top) and wall-normal (bottom) velocity contours. Color map: experimental data; lines: WMLES.

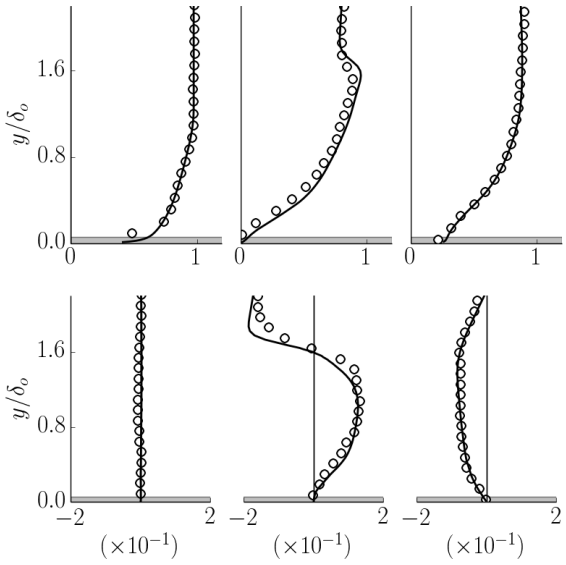

(b) Mean streamwise (top) and wall-normal (bottom) velocity profiles at x/δ_0 = 2.1, 5.4 and 7.9, from left to right. Symbols: experimental data; lines: WMLES.

Fig. 11 Mean velocity contours (a) and one-dimensional, wall-normal profiles (b) near the interaction of an oblique shock wave and a turbulent boundary layer developed inside a nearly square duct. Data taken at a plane near the spanwise center of the duct. Velocities are normalized with the unperturbed mean streamwise velocity at the center of the duct upstream the oblique shock. Adapted from Bermejo-Moreno *et al.* (2014).

As mentioned above, Hickel *et al.* (2012) found a convincing balance between these terms (outside the viscous layer) at multiple streamwise locations in both a shock/boundary-layer interaction and an incompressible separation bubble. And, in Catalano *et al.* (2003)'s application of their wall-stress-modeled LES to a cylinder flow (which retained the pressure-gradient but discarded the convective term), the computed skin friction coefficient was overpredicted by a factor of 3 on the front side of the cylinder. This is a region of strong acceleration, thus very large (and positive) $\partial(uu)/\partial x$ and almost equally large (but negative) $(1/\rho)\partial p/\partial x$. Retaining only the latter in Eqn. (1) causes the velocity profile to have unphysically large curvature, which leads to unphysically large τ_w. This is consistent with (and arguably explains) their very large overprediction of the skin friction coefficient c_f.

So, if we want to retain one term on the left hand side of Eqn. (1), then we must retain them all. Given that, the perhaps only possible way towards a wall-model without wall-parallel derivatives would be to somehow approximate the convective terms.

Hickel *et al.* (2012) tried doing this in two different ways. First, by assuming that $\partial(uu_j)/\partial x_j$ has the same shape in y as the velocity to some power, i.e., that $\partial(uu_j)/\partial x_j \sim u^\alpha$. By matching this term to the known LES values at the top of the wall-modeled layer (i.e., at $y = h_{\text{wm}}$), this closed the system. This worked very well in *a priori* tests, but not nearly as well when actually trying to predict τ_w given an LES solution at $y = h_{\text{wm}}$. Their second attempt was directly inspired by the approximate balance between convection and pressure-gradient outside the viscous layer, assuming that $\partial(uu_j)/\partial x_j$ was equal to the pressure-gradient above some y^+ (i.e., a perfect equilibrium model) but that it then decreased linearly towards 0 at the wall. This attempt worked better, giving reasonable results for both test cases.

More recently, Yang *et al.* (2015) assumed a parametrized shape function for the velocity in the wall-model, and then analytically integrated the momentum equation in the vertical direction. They then used different constraints to determine the parametrized shape at each time step, including the matching with the LES velocity at $y = h_{\text{wm}}$. The model was tested on channel flow with and without roughness as well as on the flow over an array of wall-mounted cubes. Since the model includes the non-equilibrium terms in a consistent manner, it has the potential to be accurate even on more complex flows like the separation over a smooth surface.

3.5. The unresolved scales in the inner layer

Wall-modeling in LES aims to eliminate the need to resolve the small and fast scales in the inner layer. Accordingly, wall-stress-models are designed specifically to have zero spectral content at frequencies associated with inner layer mo-

tions. Any information at high frequencies, whether fluctuating wall stress, wall pressure, or velocities, is neither needed nor desired when advancing the WMLES equations in time.

However, such information of near-wall fluctuations at unresolved scales can be very useful in the accurate prediction of physical phenomena that are coupled with wall turbulence, including sound generation, mixing, combustion, radiation and fluid-structure interaction. For example, a wall-modeled LES can at best predict the spectrum of radiated sound up to outer-layer frequencies of order u_τ/δ. Variations of the instantaneous fluctuating near-wall temperature can have a significant impact on the chemical reactions and species concentration of turbulent flows involving combustion, as well as on its interaction with radiation. Likewise, fluctuations of the wall shear-stress (found to exceed five times the mean value by Örlü & Schlatter, 2011) can severely affect the solid wall structure in some applications (e.g., mobilization of particles resting on the wall surface).

3.5.1. Multi-scale interactions between the inner and outer layers – physical picture The degree (and directionality) of interdependence between the near-wall (unresolved) scales and the larger (resolved) scales in the outer layer is critical to justify, from a hydrodynamical standpoint, the suitability of WMLES. Multiple studies in the literature are found to support Townsend (1976)'s outer-layer similarity hypothesis, by which the wall shear stress and wall impermeability condition are enough to define the outer flow of the boundary layer, without the need of imposing the no-slip condition, and thus independently of the viscous sublayer. Besides studies of different smooth and rough walls leading to similar log-layers (Perry & Abell, 1977; Jiménez, 2004; Flores & Jimenez, 2006), recently Mizuno & Jiménez (2013) proved through numerical experiments that a logarithmic layer can still be maintained when the inner layer is substituted by an off-wall boundary condition with velocities replaced by rescaled and shifted copies of those at an interior reference plane, thus suppressing the viscous and buffer layers and the near-wall maximum found in the energy spectrum. Testing Townsend's hypothesis directly, Chung *et al.* (2014) compared channel flow DNS at moderate Reynolds numbers with no-slip versus shear-stress boundary conditions, observing that the outer flow (even high-order statistics) remains largely independent of the viscous sublayer. Furthermore, the LES of Lee *et al.* (2013), performed with a mean wall shear stress boundary condition and under very coarse near-wall grid resolution, provide evidence that fluctuations of wall shear stress are not essential for accurate predictions of the logarithmic velocity profile and low-order statistics.

Early numerical studies (Jimenez & Moin, 1991; Hamilton *et al.*, 1995; Jiménez & Pinelli, 1999) identified the near-wall turbulent motions as the outcome of autonomous processes that are independent of the outer turbulence, and that are very similar among all smooth wall-bounded turbulence (pipe, channel and boundary layer), whose only differences lie on the larger-scale, geometry-dependent, motions. On the other hand, large-scale motions observed in experiments (Kim & Adrian, 1999) and simulations (del Alamo & Jimenez, 2003; Abe *et al.*, 2004; Iwamoto *et al.*, 2005) to develop in the outer layer are known to deeply penetrate into the near-wall region (De Graaff & Eaton, 2000; Hutchins & Marusic, 2007) and influence significantly the near-wall flow through an apparent amplitude modulation of the underlying small-scale fluctuations (Mathis *et al.*, 2009; Chung & McKeon, 2010). There is now extensive evidence that the near-wall cycle is also influenced by large-scale modulating events, increasingly so with higher Reynolds numbers: the so-called superstructures are not simply superimposed onto the near-wall region but appear to actively modulate the production of near-wall scales (Hutchins & Marusic, 2007). It has also been observed that the log-layer dynamics play a crucial role in the generation of turbulent skin friction (Hwang, 2013), and that the contribution of narrow, near-wall motions to the total turbulent skin friction decays with increasing Reynolds number.

Supported by this conceptual view of a universal inner layer that is modified by the modulation and superposition of outer, large-scale motions dictated by the geometry or pressure gradient, Marusic *et al.* (2010) and Mathis *et al.* (2011) developed a model for inner-outer scale interactions (IOSI model) that predicts the statistics of the streamwise velocity fluctuations in the inner layer from a measured large-scale velocity signature taken at an outer position in the logarithmic layer (see Fig. 12). The universality of the model was suggested for four types of wall-bounded flows (channel, pipe, zero-pressure-gradient and adverse-pressure-gradient turbulent boundary layers), although modifications of the model parameters are needed for the adverse-pressure-gradient turbulent boundary layer, which has a stronger effect of the outer scales on the near-wall scales than in the zero-pressure-gradient turbulent boundary layer. Note that the notion of universality implies that the near-wall small-scale motions are not directly dependent on the Reynolds number, but the influence and intensity of the large-scale events in the logarithmic region increases with the Reynolds number. Thus, the model parameters can be determined (i.e., calibrated) at an arbitrarily chosen Reynolds number. Predictions of this model agree very well with actual experimental measurements and direct numerical simulations. Helm & Pino Martin (2013) applied the IOSI model to compressible turbulent boundary layers in supersonic and hypersonic flow conditions and extended it to include near-wall predictions of density and temperature fluctuations, finding good agreement with

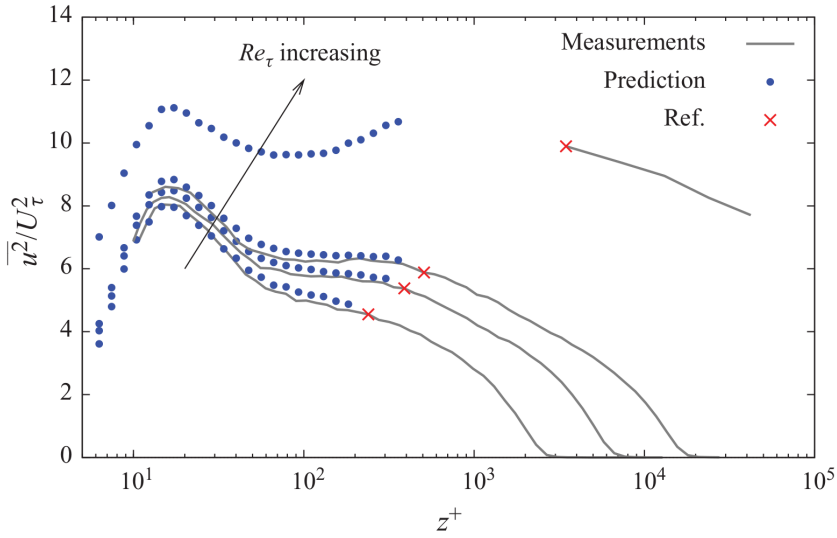

Fig. 12 Comparison of experimental measurements (solid line) and IOSI model predictions of the wall-normal profile of streamwise turbulence intensity ($\overline{u^2}/U_\tau^2$) for increasing Reynolds number. The red crosses mark the outer locations where the large-scale velocity signature feeding the IOSI model is taken. Reproduced from Mathis *et al.* (2011).

DNS data. Mathis *et al.* (2013) extended the IOSI model to also reconstruct the fluctuating (streamwise component of the) wall-shear stress.

3.5.2. Application to WMLES – the distinction between one- and two-way coupling The IOSI model (or any other model for the unresolved scales in the inner layer) is potentially quite useful in the context of wall-modeled LES. The role played by such a model depends on the physics of the flow and on what quantities one is interested in. To examine this issue, we consider a wall-stress-modeled LES that satisfies the accuracy and grid-resolution criteria given in section 3.2, and specifically consider how the WMLES evolution equations are coupled (or not) to the unresolved motions in the inner layer (as predicted by the IOSI or similar model).

In the scenario considered here the IOSI model depends on the WMLES, since it makes predictions about the unresolved scales based on information about the large, outer-layer scales.

For a turbulent boundary layer with no additional physics involved, there is no coupling from the IOSI model to the WMLES evolution equations. The WMLES equations are designed, on purpose, to avoid resolving the smallest scales, and they only require information about the mean (or, at the very least, very low-frequency) wall quantities (τ_w, q_w, etc). In these one-way coupled situations, the IOSI model would be a post-processing element: it would not affect the time-integration of the WMLES, but it could enhance or complement the results. Examples where this could be useful include the prediction of sound (the IOSI model would contribute to the highest frequencies), the prediction of mobilization of sand particles on the bottom of a river (mobilization requires the shear stress to exceed some threshold), and the forcing of high-frequency modes in a fluid-structure interaction problem; in all cases assuming there is no feedback on the fluid motion.

In addition to these one-way coupled situations, one can also envision flow problems with two-way coupling, i.e., where the unresolved motions predicted by the IOSI model *would* affect the WMLES evolution equations. For example, in turbulent combustion near walls, the chemical reactions are strongly affected by near-wall small-scale fluctuations, as shown by Gruber *et al.* (2010) in their DNS studies of the interaction of a turbulent flame with turbulent boundary layer. Those changes lead to modifications of the flame speed and stretch, a change of the combustion regime near the wall, and modifications of the heat release at the wall, all of which would affect the outer flow. Likewise, several problems involving fluid-solid-structure/thermal interactions might exhibit two-way coupling, for example if small-scale fluctuations would affect the rate of ablation of a hot surface. For these types of two-way coupled problems, it may be necessary to solve the WMLES and the IOSI (or similar) model in a tightly coupled manner.

4. Summary and future directions

Wall-modeled LES (WMLES) has now been around for 45 years and has reached a certain level of maturity, yet there

are still obstacles to overcome before WMLES becomes an everyday tool in applied engineering. In this final section, we try to identify some of the main challenges that lie ahead along with some thoughts on how to tackle them.

4.1. Wall-modeled LES – what it is, what it's not, and what we can reasonably expect

Wall-modeled LES is different from both the original version of DES ("DES97"; Spalart *et al.*, 1997) and traditional (wall-resolved) LES. By resolving the outer part of the boundary layer, WMLES has the potential to be much more accurate than DES97, especially in situations where the boundary layer is far from equilibrium (accelerating, decelerating, turning, separating, ...). However, it is also clear that properly performed WMLES is *not* computationally cheap – it can be orders of magnitude cheaper than LES, but it is still orders of magnitude more expensive than both DES97 and RANS.

WMLES has sometimes suffered from unreasonable expectations in the LES community, specifically the expectation that a wall-model should lead to affordable LES. This expectation seems to stem from a failure to fully appreciate the need to accurately resolve the outer layer: simply put, using a wall-model in LES alleviates the need to resolve the *inner* layer, but is not a license to poorly resolve the *outer* layer.

Moving forward, we need to recognize both the (significant) promises and inherent limitations of wall-modeled LES.

4.2. The importance of showing grid-convergence and, if possible, testing different numerics

The whole idea behind LES is to avoid having to resolve some turbulent motions, and thus by definition the grid has an effect on the results. This is taken one step further in wall-modeled LES, where we create the grid to avoid resolving some of the energetic and dynamically important motions. Since the grid has a direct effect on the results, it is *mandatory* to test all wall-modeled LES approaches on different grids: both by refining the grid *and* by modifying the aspect ratio of the grid. We remind the reader of Figs. 5 and 9 which show the importance of demonstrating grid-convergence for typical hybrid LES/RANS and wall-stress-modeled methods; note specifically that the results in Fig. 5 are best (smallest log-layer mismatch) for the coarsest grid.

When assessing the sensitivity to the grid, one must vary the grid-spacing in *outer* units – the grid-spacing in inner (viscous, or "plus") units is irrelevant in wall-modeled LES. For example, it is common to use the same grid in outer units and then vary the Reynolds number to produce variation in the Δx_i^+; this tests the sensitivity to the Reynolds number but *not* to the grid-spacing itself.

In addition to the mandatory variation of the grid-spacing and the grid-anisotropy, it is extremely useful to also test any WMLES method in different codes using different numerical methods, if possible. The discussion in section 3.2 has hopefully convinced the reader that the numerical errors are important and hard to avoid – the direct corollary to this observation is that a flawed model may produce "perfect" results by introducing errors that exactly cancel those present in the outer layer LES. For example, since most codes/numerics produce a positive log-layer mismatch, any modeling modification that by itself would produce a negative mismatch will lead to "improved" results.

The major point here is that wall-modeled LES has, by its very nature (underresolved by design in a region where the turbulence is highly anisotropic), a potentially strong sensitivity to both the grid and the numerics, in principle more so than many other areas or applications of LES (e.g., free shear flows). It is instructive to consider the area of DES, for which the issue of "grid-induced separation" was detected and documented rather early (Menter & Kuntz, 2004; Spalart, 2009). This problem is (somewhat simplistically) caused by the strong connection between the grid and the modeling (the eddy-viscosity) in the original formulation of DES97, and, more importantly in our context, appears only for certain grid-spacings and grid-anisotropies. Given this experience in the DES field, it would seem prudent to assume (until proven otherwise) that every WMLES approach may be sensitive to the grid-spacing and the grid-anisotropy.

4.3. Challenge #1: separated and other non-equilibrium flows

While equilibrium wall-models are much better suited to predicting non-equilibrium flows than they are often given credit for, there is still work to be done on developing a robust approach to, first and foremost, separated flows.

The first real need for this effort is a sufficiently well-defined experimental validation problem. First, the most important validation point in a separated flow is the skin friction profile, which is likely to be estimated from a Clauser chart at high Reynolds numbers – a process which assumes the existence and validity of a log-law (Wei *et al.*, 2005). Secondly, the uncertainties in many experimental parameters (inflow velocity and turbulent stress profiles, spanwise confinement effects, etc) introduce uncertainties in the output results. Only such discrepancies in the WMLES results that are sufficiently larger than those uncertainties are meaningful; in practice, the differences between different wall-modeling approaches may be smaller than that. This was partially the case in Kawai & Larsson (2013), who computed a shock/boundary-

layer interaction at $Re_\theta \approx 50,000$ in order to validate their proposed non-equilibrium wall-model. While the proposed non-equilibrium wall-modeled LES results were in excellent agreement with the experimental data, the results using an equilibrium wall-model were also within the experimental uncertainties.

In summary, combining the experimental uncertainties with the lack of proven grid-convergence in most studies, one must conclude that there has not yet been a truly convincing and conclusive demonstration of any superiority of non-equilibrium over equilibrium wall-stress-models in LES. Performing such a conclusive demonstration is a high priority in the field, regardless of the eventual conclusion from it. If it turns out to be important to model the convection/pressure-gradient terms for these flows, then approaches like that of Yang *et al.* (2015) seem particularly promising: i.e., the inclusion of convection/pressure-gradient in a manner consistent with the Bernoulli equation while yet requiring at most the solution of an ODE in the wall-normal direction.

4.4. Challenge #2: multi-physics effects in the inner layer

The vast majority of developments and assessments of wall-stress-modeled LES has been for flows with "canonical" physics effects, and there is a large opportunity for work on flows with substantial additional physics occurring in the inner layer. One example is chemical reactions, especially for hydrogen fuels which can burn very close to the wall. Another is in the modeling of the variance of a passive scalar, for which it is plausible that the vigorous inner layer turbulence may affect the scalar variance. When confronted by the need to model scalar variance in wall-modeled LES, Larsson *et al.* (2015) simply resorted to the (somewhat desperate) assumption of it having zero wall-normal gradient in the log-layer; surely one can do better than that. A third example is the inclusion of radiation effects, as done by Zhang *et al.* (2013).

These and other cases may exhibit both one- and two-way coupling, both of which require modeling-advances beyond the current state-of-the-art. More broadly, the presence of multi-physics effects raises the possibility of situations where the wall-stress-model needs to return more information than merely the wall fluxes (of momentum, heat, scalars, etc). The present paradigm in wall-stress-modeling is essentially based on a finite-volume approach to the LES, in which only the wall fluxes are needed (if any volumetric source terms exist, they should then be included in both the wall-model and the LES itself, of course). An interesting question going forward is whether there are multi-physics phenomena for which the unresolved inner layer processes cause important effects on the volumetric LES (resolved or subgrid) which are not included in the modeled wall flux.

4.5. Challenge #3: adaptive or automated modeling

The thickness of the wall-modeled layer h_{wm} is the main modeling parameter in wall-modeled LES. The obvious problem, of course, is that h_{wm} should be chosen as a fraction of the boundary layer thickness δ, which is unknown *a priori*. This is a problem in applied engineering situations, where the speed of the complete simulation process is important. We should not be too critical of WMLES: the situation is basically the same for RANS, DES and traditional LES. The higher cost of WMLES compared to RANS and DES97, however, means that there is less room for trial-and-error when creating the grid and defining the problem (i.e., choosing the h_{wm} distribution in space). Of these, the definition of h_{wm} is the more pressing problem, since the grid can be designed following the criteria in section 3.2 once h_{wm} has been set.

Little has been done in this area, and thus the field is open to new ideas. For complex flows, the solution will likely be iterative: a preliminary simulation that allows for the definition of h_{wm} followed by a more accurate simulation. In practice, this may be best implemented using RANS in the preliminary step.

A slightly different issue is the problem of how to treat regions where the grid is sufficiently good for traditional LES. The immediate answer is that the wall-model should be switched off in those regions, but this is not trivial to achieve in practice. Specifically, there exists multiple combinations of grid-resolutions in all three directions (sufficient for traditional LES or not) and the state of the boundary layer (turbulent or not), and an adaptive method would need to make the right "decision" in all possible scenarios. In addition, one must consider the possibility of hysteresis. This problem was addressed in the context of hybrid LES/RANS by Abe (2014), who devised a LES-RANS blending function that produces pure LES behavior for sufficiently fine grids; a similar approach is needed in wall-stress-modeled LES.

Acknowledgments

This paper contains work done by the authors when they were at the Center for Turbulence Research as well as more recent work done at their present institutions. Prior to about 2012, the work was supported in part by the NASA Fixed-

Wing program, the AFOSR Turbulence program and the DOE PSAAP program. More recently, JL has been supported by NSF grant CBET-1453633, while SK has been supported by JSPS Grant-in-Aid for Young Scientists (A) KAKENHI 26709066.

References

Abe, H., Kawamura, H. & Choi, H. 2004 Very large-scale structures and their effects on the wall shear-stress fluctuations in a turbulent channel flow up to reτ= 640. *J. Fluids Engr.* **126** (5), 835–843.

Abe, K. 2014 An advanced switching parameter for a hybrid LES/RANS model considering the characteristics of near-wall turbulent length scales. *Theor. Comp. Fluid Dyn.* **28**, 499–519.

Baggett, J. S. 1998 On the feasibility of merging LES with RANS for the near-wall region of attached turbulent flows. In *Annu. Res. Briefs*, pp. 267–277. Center for Turbulence Research.

Balaras, E., Benocci, C. & Piomelli, U. 1996 Two-layer approximate boundary conditions for large-eddy simulations. *AIAA J.* **34** (6), 1111–1119.

Baurle, R. A., Tam, C.-J., Edwards, J. R. & Hassan, H. A. 2003 Hybrid simulation approach for cavity flows: blending, algorithm, and boundary treatment issues. *AIAA J.* **41** (8), 1463–1480.

Bermejo-Moreno, I., Campo, L., Larsson, J., Bodart, J., Helmer, D. & Eaton, J. 2014 Confinement effects in shock wave/turbulent boundary layer interactions through wall-modeled large-eddy simulations. *J. Fluid Mech.* **758**, 5–62.

Bodart, J. & Larsson, J. 2011 Wall-modeled large eddy simulation in complex geometries with application to high-lift devices. In *Annu. Res. Briefs*, pp. 37–48. Center for Turbulence Research.

Bodart, J. & Larsson, J. 2012 Sensor-based computation of transitional flows using wall-modeled large eddy simulation. In *Annu. Res. Briefs*, pp. 229–240. Center for Turbulence Research.

Bose, S. T. & Moin, P. 2014 A dynamic slip boundary condition for wall-modeled large-eddy simulation. *Phys. Fluids* **26**, 015104.

Brasseur, J. G. & Wei, T. 2010 Designing large-eddy simulation of the turbulent boundary layer to capture law-of-the-wall scaling. *Phys. Fluids* **22**, 021303.

Cabot, W. & Moin, P. 1999 Approximate wall boundary conditions in the large-eddy simulation of high Reynolds number flow. *Flow Turbul. Combust.* **63**, 269–291.

Catalano, P., Wang, M., Iaccarino, G. & Moin, P. 2003 Numerical simulation of the flow around a circular cylinder at high Reynolds numbers. *Int. J. Heat Fluid Flow* **24**, 463–469.

Chapman, D. R. 1979 Computational aerodynamics development and outlook. *AIAA J.* **17** (12), 1293–1313.

Chen, S., Xia, Z., Pei, S., Wang, J., Yang, Y., Xiao, Z. & Shi, Y. 2012 Reynolds-stress-constrained large-eddy simulation of wall-bounded turbulent flows. *J. Fluid Mech.* **703**, 1–28.

Chen, Z. L., Hickel, S., Devesa, A., Berland, J. & Adams, N. A. 2014 Wall modeling for implicit large-eddy simulation and immersed-interface methods. *Theor. Comp. Fluid Dyn.* **28**, 1–21.

Choi, H. & Moin, P. 2012 Grid-point requirements for large eddy simulation: Chapman's estimates revisited. *Phys. Fluids* **24**, 011702.

Choi, J.-I., Edwards, J. R. & Baurle, R. A. 2009 Compressible boundary-layer predictions at high Reynolds number using hybrid LES/RANS methods. *AIAA J.* **47** (9), 2179–2193.

Chung, D & McKeon, BJ 2010 Large-eddy simulation of large-scale structures in long channel flow. *J. Fluid Mech.* **661**, 341–364.

Chung, D., Monty, J.P. & Ooi, A. 2014 An idealised assessment of Townsends outer-layer similarity hypothesis for wall turbulence. *J. Fluid Mech.* **742**, R3.

Coleman, G. N., Garbaruk, A. & Spalart, P. R. 2015 Direct numerical simulation, theories and modelling of wall turbulence with a range of pressure gradients. *Flow Turbul. Combust.* **95**, 261–276.

Craft, T. J., Gant, S. E., Iacovides, H. & Launder, B. E. 2004 A new wall function strategy for complex turbulent flows. *Num. Heat Transfer B.* **45**, 301–318.

Davidson, L. & Billson, M. 2006 Hybrid LES-RANS using synthesized turbulent fluctuations for forcing in the interface region. *Int. J. Heat Fluid Flow* **27** (6), 1028–1042.

Davidson, L. & Dahlström, S. 2005 Hybrid LES-RANS: an approach to make LES applicable at high Reynolds number. *Int. J. CFD* **19** (6), 415–427.

Davidson, L. & Peng, S. H. 2003 Hybrid LES-RANS modelling: a one-equation SGS model combined with a $k-\omega$ model for predicting recirculating flows. *Int. J. Num. Meth. Fluids* **43**, 1003–1018.

De Graaff, D.B. & Eaton, J.K. 2000 Reynolds-number scaling of the flat-plate turbulent boundary layer. *J. Fluid Mech.* **422**, 319–346.

Deardorff, J. W. 1970 A numerical study of three-dimensional turbulent channel flow at large Reynolds numbers. *J. Fluid Mech.* **41**, 453–480.

del Alamo, J. C. & Jimenez, J. 2003 Spectra of the very large anisotropic scales in turbulent channels. *Phys. Fluids* **15** (6), L41–L43.

Duprat, C., Balarac, G., Metais, O., Congedo, P. M. & Brugiere, O. 2011 A wall-layer model for large-eddy simulations of turbulent flows with/out pressure gradient. *Phys. Fluids* **23**, 015101.

Flores, O. & Jimenez, J. 2006 Effect of wall-boundary disturbances on turbulent channel flows. *J. Fluid Mech.* **566**, 357–376.

Germano, M. 2004 Properties of the hybrid RANS/LES filter. *Theor. Comp. Fluid Dyn.* **17**, 225–331.

Gruber, A, Sankaran, R, Hawkes, ER & Chen, JH 2010 Turbulent flame–wall interaction: a direct numerical simulation study. *J. Fluid Mech.* **658**, 5–32.

Hamba, F. 2009 Log-layer mismatch and commutation error in hybrid RANS/LES simulation of channel flow. *Int. J. Heat Fluid Flow* **30**, 20–31.

Hamilton, J.M., Kim, J. & Waleffe, F. 1995 Regeneration mechanisms of near-wall turbulence structures. *J. Fluid Mech.* **287**, 317–348.

Helm, C. & Pino Martin, M. 2013 Predictive Inner-Outer Model for Turbulent Boundary Layers Applied to Hypersonic DNS Data. *AIAA 2013* **265**.

Hickel, S., Touber, E., Bodart, J. & Larsson, J. 2012 A parametrized non-equilibrium wall-model for large-eddy simulations. In *Proceedings of the Summer Program*, pp. 127–136. Center for Turbulence Research.

Hoffmann, G. & Benocci, C. 1995 Approximate wall boundary conditions for large eddy simulations. In *Advances in turbulence V: Proceedings of the 5th European Turbulence Conference*.

Hoyas, S. & Jimenez, J. 2008 Reynolds number effects on the Reynolds-stress budgets in turbulent channels. *Phys. Fluids* **20**, 101511.

Hutchins, N. & Marusic, I. 2007 Large-scale influences in near-wall turbulence. *Phil. Trans. R. Soc. A* **365** (1852), 647–664.

Hwang, Y. 2013 Near-wall turbulent fluctuations in the absence of wide outer motions. *J. Fluid Mech.* **723**, 264–288.

Iwamoto, Kaoru, Kasagi, Nobuhide & Suzuki, Yuji 2005 Direct numerical simulation of turbulent channel flow at Re_τ= 2320. In *Proc. 6th Symp. Smart Control of Turbulence*, pp. 327–333.

Jiménez, J. 2004 Turbulent flow over rough walls. *Annual Review of Fluid Mechanics* **36**, 173–196.

Jimenez, J. 2012 Cascades in wall-bounded turbulence. *Annu. Rev. Fluid Mech.* **44**, 27–45.

Jimenez, J. & Moin, P. 1991 The minimal flow unit in near-wall turbulence. *J. Fluid Mech.* **225**, 213–240.

Jiménez, J. & Pinelli, A. 1999 The autonomous cycle of near-wall turbulence. *J. Fluid Mech.* **389**, 335–359.

Kawai, S. & Larsson, J. 2012 Wall-modeling in large eddy simulation: length scales, grid resolution and accuracy. *Phys. Fluids* **24**, 015105.

Kawai, S. & Larsson, J. 2013 Dynamic non-equilibrium wall-modeling for large eddy simulation at high Reynolds numbers. *Phys. Fluids* **25**, 015105.

Keating, A. & Piomelli, U. 2006 A dynamic stochastic forcing method as a wall-layer model for large-eddy simulation. *J. Turbul.* **7**, N12.

Kim, K.C. & Adrian, R.J. 1999 Very large-scale motion in the outer layer. *Phys. Fluids* **11** (2), 417–422.

Larsson, J. 2006 Towards large eddy simulation of boundary layer flows at high Reynolds number: statistical modeling of the inner layer. PhD thesis. University of Waterloo.

Larsson, J., Laurence, S. J., Bermejo-Moreno, I., Bodart, J., Karl, S. & Vicquelin, R. 2015 Incipient thermal choking and stable shock-train formation in the heat-release region of a scramjet combustor. Part II: Large eddy simulations. *Combust. Flame* **162**, 907–920.

Larsson, J., Lien, F. S. & Yee, E. 2006 Feedback-controlled forcing in hybrid LES/RANS. *Int. J. CFD* **20** (10), 687–699.

Lee, J., Cho, M. & Choi, H. 2013 Large eddy simulations of turbulent channel and boundary layer flows at high Reynolds number with mean wall shear stress boundary condition. *Phys. Fluids* **25**, 110808.

Marusic, I., Mathis, R. & Hutchins, N. 2010 Predictive model for wall-bounded turbulent flow. *Science* **329** (5988), 193–196.

Mathis, R., Hutchins, N. & Marusic, I. 2009 Large-scale amplitude modulation of the small-scale structures in turbulent boundary layers. *J. Fluid Mech.* **628**, 311–337.

Mathis, R., Hutchins, N. & Marusic, I. 2011 A predictive inner–outer model for streamwise turbulence statistics in wall-bounded flows. *J. Fluid Mech.* **681**, 537–566.

Mathis, R., Marusic, I., Chernyshenko, S.I. & Hutchins, N. 2013 Estimating wall-shear-stress fluctuations given an outer region input. *J. Fluid Mech.* **715**, 163–180.

Meneveau, C., Lund, T. S. & Cabot, W. H. 1996 A Lagrangian dynamic subgrid-scale model of turbulence. *J. Fluid Mech.* **319**, 353–385.

Menter, F. R. & Kuntz, M. 2004 Adaptation of eddy-viscosity turbulence models to unsteady separated flow behind vehicles. In Lecture Notes in Applied and Computational Mechanics, vol 19, 339–352.

Mizuno, Y. & Jiménez, J. 2013 Wall turbulence without walls. *J. Fluid Mech.* **723**, 429–455.

Nicoud, F., Baggett, J. S., Moin, P. & Cabot, W. 2001 Large eddy simulation wall-modeling based on suboptimal control theory and linear stochastic estimation. *Phys. Fluids* **13** (10), 2968–2984.

Nikitin, N. V., Nicoud, F., Wasistho, B., Squires, K. D. & Spalart, P. R. 2000 An approach to wall modeling in large-eddy simulations. *Phys. Fluids* **12** (7), 1629–1632.

Örlü, R. & Schlatter, P. 2011 On the fluctuating wall-shear stress in zero pressure-gradient turbulent boundary layer flows. *Phys. Fluids* **23** (2), 1704.

Park, G. I. & Moin, P. 2014 An improved dynamic non-equilibrium wall-model for large eddy simulation. *Phys. Fluids* **26**, 015108.

Perry, A.E. & Abell, C.J. 1977 Asymptotic similarity of turbulence structures in smooth-and rough-walled pipes. *J. Fluid Mech.* **79** (04), 785–799.

Piomelli, U. 2008 Wall-layer models for large-eddy simulations. *Prog. Aero. Sci.* **44**, 437–446.

Piomelli, U. & Balaras, E. 2002 Wall-layer models for large-eddy simulations. *Annu. Rev. Fluid Mech.* **34**, 349–374.

Piomelli, U., Balaras, E., Pasinato, H., Squires, K. D. & Spalart, P. R. 2003 The inner-outer layer interface in large-eddy simulations with wall-layer models. *Int. J. Heat Fluid Flow* **24**, 538–550.

Piomelli, U., Ferziger, J., Moin, P. & Kim, J. 1989 New approximate boundary conditions for large eddy simulations of wall-bounded flows. *Phys. Fluids A* **1** (6), 1061–1068.

Rajamani, B. & Kim, J. 2010 A hybrid-filter approach to turbulence simulation. *Flow Turbul. Combust.* **85**, 421–441.

Sagaut, P. 2006 *Large eddy simulation for incompressible flows*. Springer Verlag.

Sayadi, T., Hamman, C. W. & Moin, P. 2013 Direct numerical simulation of complete H-type and K-type transitions with implications for the dynamics of turbulent boundary layers. *J. Fluid Mech.* **724**, 480–509.

Schumann, U. 1975 Subgrid scale model for finite difference simulations of turbulent flows in plane channels and annuli. *J. Comput. Phys.* **18**, 376–404.

Shur, M. L., Spalart, P. R., Strelets, M. K. & Travin, A. K. 2008 A hybrid RANS-LES approach with delayed-DES and wall-modeled LES capabilities. *Int. J. Heat Fluid Flow* **29**, 1638–1649.

Souverein, L. J., Dupont, P., Debieve, J. F., Dussauge, J. P., van Oudheusden, B. W. & Scarano, F. 2010 Effect of interaction strength on unsteadiness in turbulent shock-wave-induced separations. *AIAA J.* **48** (7), 1440–1493.

Spalart, P. R. 2009 Detached-eddy simulation. *Annu. Rev. Fluid Mech.* **41**, 181–202.

Spalart, P. R., Jou, W.-H., Strelets, M. & Allmaras, S. R. 1997 Comments on the feasibility of LES for wings, and on a hybrid RANS/LES approach. In *Advances in DNS/LES* (ed. C. Liu & Z. Liu). Greyden, Columbus, OH.

Temmerman, L., Hadziabdic, M., Leschziner, M. & Hanjalic, K. 2005 A hybrid two-layer URANS-LES approach for large eddy simulation at high Reynolds numbers. *Int. J. Heat Fluid Flow* **26**, 173–190.

Templeton, J. A., Wang, M. & Moin, P. 2006 An efficient wall model for large-eddy simulation based on optimal control theory. *Phys. Fluids* **18**, 025101.

Templeton, J. A., Wang, M. & Moin, P. 2008 A predictive wall model for large-eddy simulation based on optimal control techniques. *Phys. Fluids* **20**, 065104.

Townsend, A. A. 1976 *The Structure of Turbulent Shear Flow*, 2nd edn. Cambridge University Press.

Wang, M. & Moin, P. 2002 Dynamic wall modeling for large-eddy simulation of complex turbulent flows. *Phys. Fluids* **14** (7), 2043–2051.

Wei, T., Schmidt, R. & McMurty, P. 2005 Comment on the Clauser chart method for determining the friction velocity. *Exp. Fluids* **38**, 695–699.

Wu, P. & Meyers, J. 2013 A constraint for the subgrid-scale stresses in the logarithmic region of high Reynolds number turbulent boundary layers: A solution to the log-layer mismatch problem. *Phys. Fluids* **25**, 015104.

Yang, X. I. A., Sadique, J., Mittal, R. & Meneveau, C. 2015 Integral wall model for large eddy simulations of wall-bounded turbulent flows. *Phys. Fluids* **27**, 025112.

Zhang, Y. F., Vicquelin, R., Gicquel, O. & Taine, J. 2013 A wall model for LES accounting for radiation effects. *Int. J. Heat Mass Trans.* **67**, 712–723.